

AD-A 128 578

REPORT NO. NADC-82253-30



NADC
Tech. Info.

IMPULSE RESPONSE OF THE OCEAN FLOOR
NONLINEAR TECHNIQUES FOR MEASUREMENT ENHANCEMENT

Thomas Gabrielson
Sensors and Avionics Technology Directorate
NAVAL AIR DEVELOPMENT CENTER
Warminster, Pennsylvania 18974

April 1983

Final Report
Task Area No.
ZR 01108

APPROVED FOR PUBLIC RELEASE; DISTRIBUTION UNLIMITED

DTIC QUALITY INSPECTED 3

Prepared by
NAVAL AIR DEVELOPMENT CENTER
Department of the Navy
Warminster, PA 18974

NOTICES

REPORT NUMBERING SYSTEM — The numbering of technical project reports issued by the Naval Air Development Center is arranged for specific identification purposes. Each number consists of the Center acronym, the calendar year in which the number was assigned, the sequence number of the report within the specific calendar year, and the official 2-digit correspondence code of the Command Office or the Functional Directorate responsible for the report. For example: Report No. NADC-78015-20 indicates the fifteenth Center report for the year 1978, and prepared by the Systems Directorate. The numerical codes are as follows:

CODE	OFFICE OR DIRECTORATE
00	Commander, Naval Air Development Center
01	Technical Director, Naval Air Development Center
02	Comptroller
10	Directorate Command Projects
20	Systems Directorate
30	Sensors & Avionics Technology Directorate
40	Communication & Navigation Technology Directorate
50	Software Computer Directorate
60	Aircraft & Crew Systems Technology Directorate
70	Planning Assessment Resources
80	Engineering Support Group

PRODUCT ENDORSEMENT — The discussion or instructions concerning commercial products herein do not constitute an endorsement by the Government nor do they convey or imply the license or right to use such products.

APPROVED BY: _____



DATE: _____

26 Apr 83

FREDERICK D. AMEEL
DEPUTY DIRECTOR, SATD

UNCLASSIFIED

SECURITY CLASSIFICATION OF THIS PAGE (When Data Entered)

REPORT DOCUMENTATION PAGE		READ INSTRUCTIONS BEFORE COMPLETING FORM
1. REPORT NUMBER NADC-82253-30	2. GOVT ACCESSION NO.	3. RECIPIENT'S CATALOG NUMBER
4. TITLE (and Subtitle) Impulse Response of the Ocean Floor: Nonlinear Techniques for Measurement Enhancement		5. TYPE OF REPORT & PERIOD COVERED Final
		6. PERFORMING ORG. REPORT NUMBER
7. AUTHOR(s) Thomas Gabrielson		8. CONTRACT OR GRANT NUMBER(s) NAVAIR DEV CEN INDEPENDENT RESEARCH FUNDS
9. PERFORMING ORGANIZATION NAME AND ADDRESS Sensors and Avionics Technology Directorate Naval Air Development Center Warminster, PA 18974		10. PROGRAM ELEMENT, PROJECT, TASK AREA & WORK UNIT NUMBERS Task Area No. ZR01108
11. CONTROLLING OFFICE NAME AND ADDRESS Naval Air Development Center Warminster, PA 18974		12. REPORT DATE April 1983
		13. NUMBER OF PAGES 55
14. MONITORING AGENCY NAME & ADDRESS (if different from Controlling Office)		15. SECURITY CLASS. (of this report) Unclassified
		15a. DECLASSIFICATION/DOWNGRADING SCHEDULE
16. DISTRIBUTION STATEMENT (of this Report) Approved for Public Release; Distribution Unlimited		
17. DISTRIBUTION STATEMENT (of the abstract entered in Block 20, if different from Report)		
18. SUPPLEMENTARY NOTES		
19. KEY WORDS (Continue on reverse side if necessary and identify by block number) Impulse Response Ocean Floor Measurements Nonlinear Techniques		
20. ABSTRACT (Continue on reverse side if necessary and identify by block number) This report describes a procedure for enhancement of impulse response measurements of the ocean floor. When these measurements are made with explosive charges, the source waveshape, being long and oscillatory, obscures much of the detail in the received signal. The effects of this source waveform can be eliminated by various forms of deconvolution, one of which - homomorphic deconvolution - is very flexible in its application and does not		

20. Abstract (Continued)

require foreknowledge of the source waveshape. Homomorphic deconvolution is a nonlinear process based on filtering the logarithmic spectrum of a signal. The special problems such as phase reconstruction and signal conditioning are discussed in the context of ocean floor measurements with explosives, and a computer code is presented that generates and checks the log-spectrum.

LIST OF FIGURES

<u>Figure</u>	<u>Page</u>
1. Basic task of nonlinear signal enhancement	4
2. Verification of deconvolution process	5
3. Complete system for ocean floor impulse response measurement and validation	6
4. Fourier transform path in complex z-plane	17
5. Construction of response for a single zero close to the Fourier transform path	19
6. Magnitude and phase changes in spectrum for transform path that passes near a zero in the z-plane	20
7. Four adjacent spectrum points of a properly-sampled real signal plotted in the complex spectrum plane	24
8. Actual spectrum progression between the four points in figure 7	25
9. Sampling of phase and phase derivative for a typical real signal sampled at the Nyquist rate	27
10. Various curve-fits of spectrum data: (a) straight line, (b) cubic curve fit to four points, (c) cubic spline fit to six points, (x) cubic spline fit to entire spectrum, (o) actual intermediate spectral points.	28
11. Example of homomorphic deconvolution of a received signal (A*B) made up of a source excitation (A) and a multipath medium response (B).	32
12. Reconstruction of explosive source waveform by log-spectral averaging	34
A-1. Configuration of Fourier and Laplace inversion paths in complex z-plane	A-3
A-2. Configuration of Fourier and Laplace inversion paths in complex s-plane. Shaded area and numbered points correspond to figure A-1	A-4

DTIC QUALITY INSPECTED 3

TABLE OF CONTENTS

<u>Title</u>	<u>Page</u>
List of Figures	ii
Summary	1
Introduction	2
The Problem	7
Deconvolution Theory	10
Applied Homomorphic Deconvolution	22
Signal Conditioning	35
Conclusions	36
References	38
Appendix A - Transform Relationships	A-1
Appendix B - Computer Code	B-1

SUMMARY

This investigation was primarily motivated by the lack of good measurements for acoustic properties of the ocean floor at low frequency (below 500 Hz). It was also an opportunistic study in that a large quantity of raw measurements of ocean floor acoustic reflectivity have already been made by NAVAIRDEV CEN in most of the major ocean regions in the world. While these measurements are not of high enough quality in their present form to provide any more than a summary measure of acoustic reflectivity, they would provide more detailed information if their time resolution could be improved significantly. Since the measurements have already been taken, this would provide a very economical means of acquiring acoustic property estimates for various ocean floor regions. The major objective was, then, to develop a technique for enhancement of ocean floor reflectivity measurements.

Because of its flexibility, a nonlinear technique known as hormomorphic deconvolution was selected for the signal enhancement process. The measurements in question were made with air-dropped sonobuoys and small explosive charges and the explosion waveform has a prolonged, oscillatory tail that obscures much of the time-domain information in the received signal. If it was not obscured by the source waveform, this received signal could be used to isolate the individual paths of propagation that are probed by a particular source-receiver geometry. By means of a nonlinear transformation basic to the enhancement process, the convolution of the source waveform and the ocean response function is reduced to an addition and then the source component is suppressed by linear filtering.

Two techniques for enhancement were developed during the course of this project. The first - a complete deconvolution process - has been computer-coded and tested on real signals with reasonable success. Although noise makes the procedure tend toward instability, most of the measurements have very high signal-to-noise ratios (a virtue of the explosive source) and, in conjunction with proper preconditioning, the process performs satisfactorily. The second process, based on averaging spectra, has proven successful in isolating the source waveshape. This technique is also nonlinear but it exploits some of the properties of the source signal itself.

As a result of their nonlinear nature, both of these techniques are dependent on the nature of the signals processed. Although the concepts developed are generally valid, it is unlikely that these processes would work without modification on other types of convolution problems. The system proposed by this investigation will, however, be thoroughly tested for its ability to enhance the type of signals available in the NAVAIRDEV CEN ocean floor reflectivity measurements. This "production" work will be done on NAVAIR block funding since the process development and preliminary testing, funded by NAVAIR DEV CEN Independent Research, has been completed.

An ancillary task of this work was the development and testing of a mathematical model and accompanying computer code for the acoustic response of the ocean floor to transient signals. This task is fully reported in the second volume of this report, published separately.¹ The model is necessary for interpretation of ocean floor reflection signals after they have been enhanced. Unless the individual propagation paths can be isolated, accurate physical property measurements cannot be made. Because this study was concerned with low frequency transient signals, existing acoustic propagation models were generally unsatisfactory.

INTRODUCTION

Since World War II, research in underwater propagation of sound has progressed from simple empirical studies to detailed numerical computations of sound fields in the inhomogeneous ocean. While this research and the attendant mathematical models have spawned sophisticated means for predicting acoustic propagation through ocean water, comparatively little progress has been made in modeling propagation through the ocean floor. In light of the importance of both advanced sensor design and fleet ASW operations in shallow water, at low frequency or for near-bottom sensors, the role of the ocean floor as a propagating medium (rather than as a simple reflector) must be understood.

This deficit in understanding is not, in general, the result of a lack of theory, but rather the consequence of a paucity of reliable measurements of the actual acoustic properties of the ocean floor. Information about the acoustic behavior of ocean sediments and basement rock is sparse and is often based on laboratory measurements at high frequency of very small, disturbed samples - measurements that cannot be extrapolated to low frequency in-situ conditions. Consequently, high quality, in-situ measurements of ocean floor acoustic properties are needed before truly representative models of this boundary can be constructed.

Over the past decade, NAVAIRDEVCON has made measurements of sound interaction with the ocean floor at approximately 250 sites around the world. Potentially, these data can be used to answer some of the fundamental questions about the influence of the bottom on sound transmission. The time resolution of these measurements is not, however, sufficient to permit direct estimation of in-bottom properties. This resolution is greatly reduced by the oscillations of the gas bubble produced by the acoustic source (an explosion). This gas bubble expands and contracts rapidly while exchanging energy between water-mass movement and gas compression until an equilibrium is reached. Ideally, a very short pulse should be used to isolate individual energy paths through the bottom but the gas bubble oscillations spread the explosion's pulse in time, thereby obscuring the individual arrivals.

Classically, a method known as inverse filtering or replica deconvolution has been used to reduce the smearing effects of the bubble oscillation. In this process, the exact waveform of the bubble oscillation must be known so that a filter can be constructed that reduces this waveform to a narrow spike.

In this investigation, a more general signal enhancement procedure is developed in which the source waveform need not be known. This method, called homomorphic deconvolution, can be used not only to reduce smearing by the source waveform, but, in another mode of operation, can be used to isolate the source waveform itself. Although inverse filtering has been successfully applied to bubble pulse reduction,² the homomorphic procedure is inherently more flexible.

Essentially, homomorphic deconvolution involves transforming the time series signal into a domain in which convolution becomes addition. Once in this additive domain, the bubble pulse, which was originally convolved with the ocean transfer function, can be suppressed by standard linear filtering procedures. Transformation back into the time domain then yields the desired ocean response as if the source has been a single, very sharp pulse.

In conjunction with this signal enhancement process, it is also necessary to develop a mathematical model of the interaction of transient acoustic signals with the ocean floor. The model must be sufficiently general to describe reflection and refraction within layered, inhomogeneous media; distortion introduced by dispersion, attenuation, and phase-shifting; and reflection of non-planar wavefronts. Without such a model, the process of interpreting the enhanced signals physically would be haphazard. Furthermore, if a model can be developed that predicts signal propagation similar to that observed in measurements, these measurements can be associated with physical phenomena and quantitative estimates of physical properties in the ocean floor can be made.

The interrelation of the different phases of this project are shown in figures 1 through 3. The fundamental task, that of deconvolving a measurement signal to generate the response of the medium, is diagrammed in figure 1. A by-product of the homomorphic technique is the ability to isolate the source waveshape. This can then be reconvolved with the medium response as shown in figure 2 to provide a measure of the quality of the deconvolution.

Once the medium response has been measured and verified, the response is translated into a physical model of the medium. This is the desired product of this research but it too must be verified. For this reason, the transient response model was developed. The model of the medium is excited by the source waveform (by computer simulation) and the resulting theoretical response can be compared to the actual received waveform. In this way the assumptions involved in building the physical model of the ocean floor can be evaluated. Thus, the procedure as a whole (figure 3) has several feedback paths to insure validity of the results.

This report summarizes the development of the deconvolution process only since that was the most time-consuming task. A companion volume¹ describes the design and operation of the model for transient response of the ocean floor and also some of the results obtained by this phase of the project.

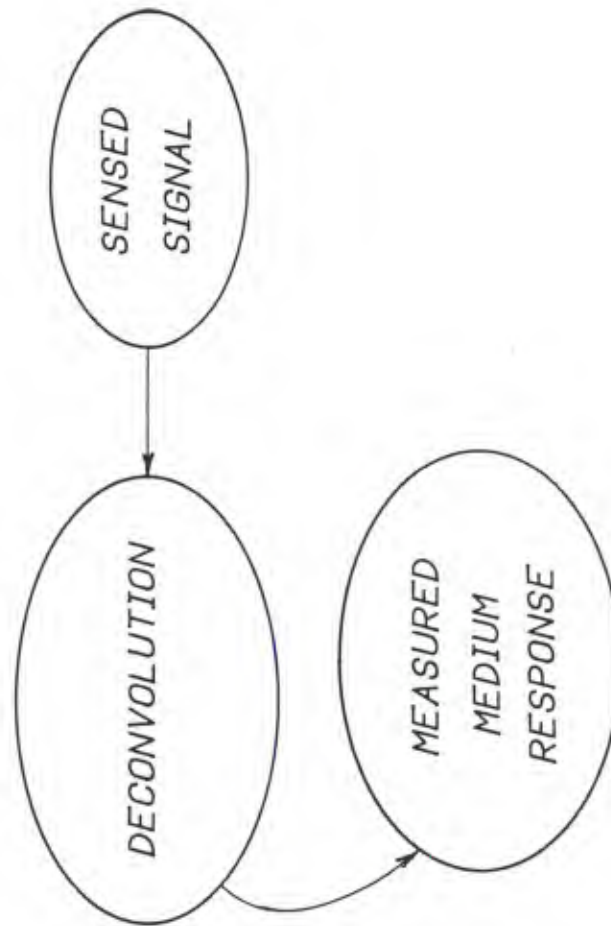


Figure 1. Basic task of nonlinear enhancement.

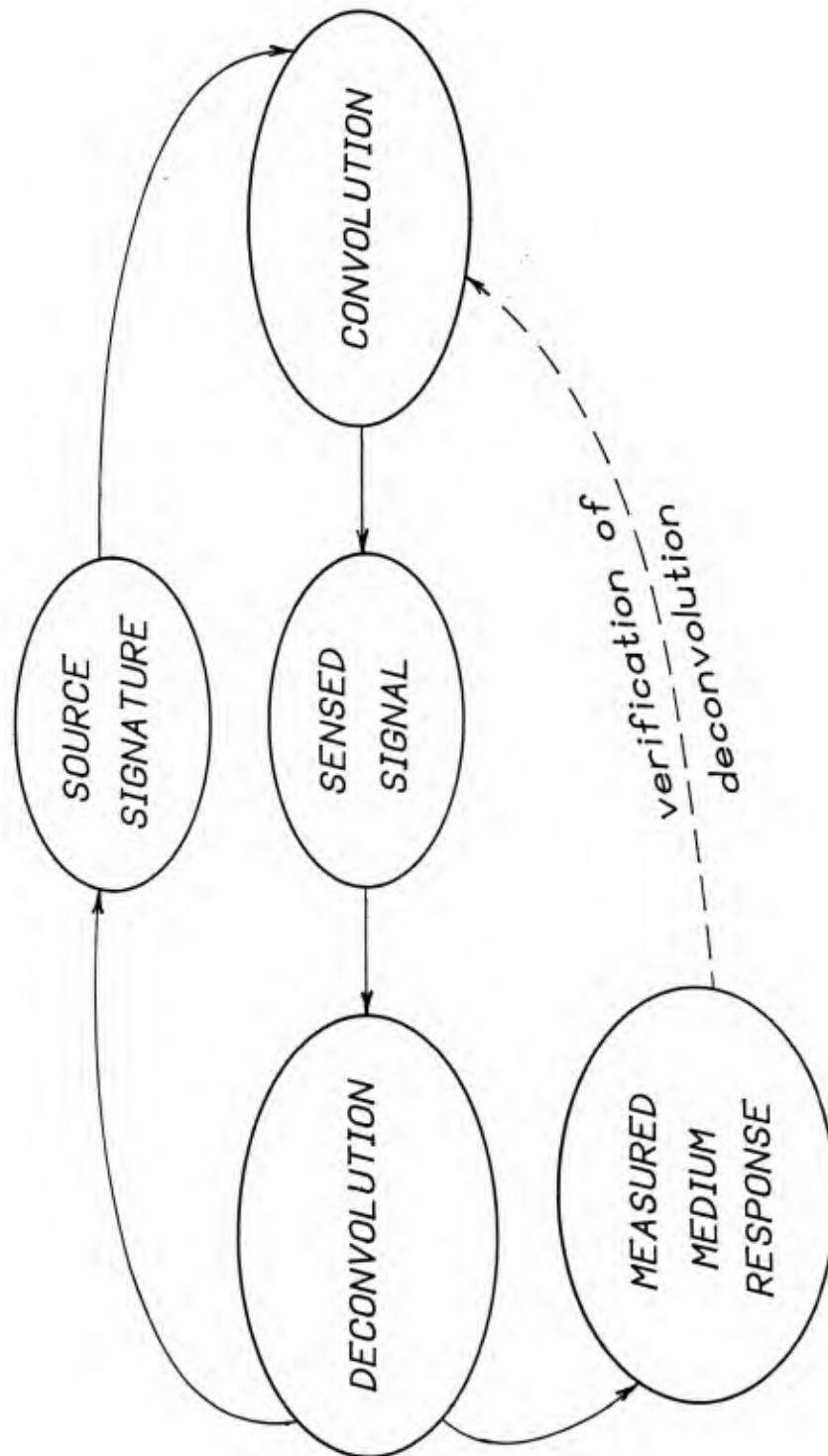


Figure 2. Verification of deconvolution process.

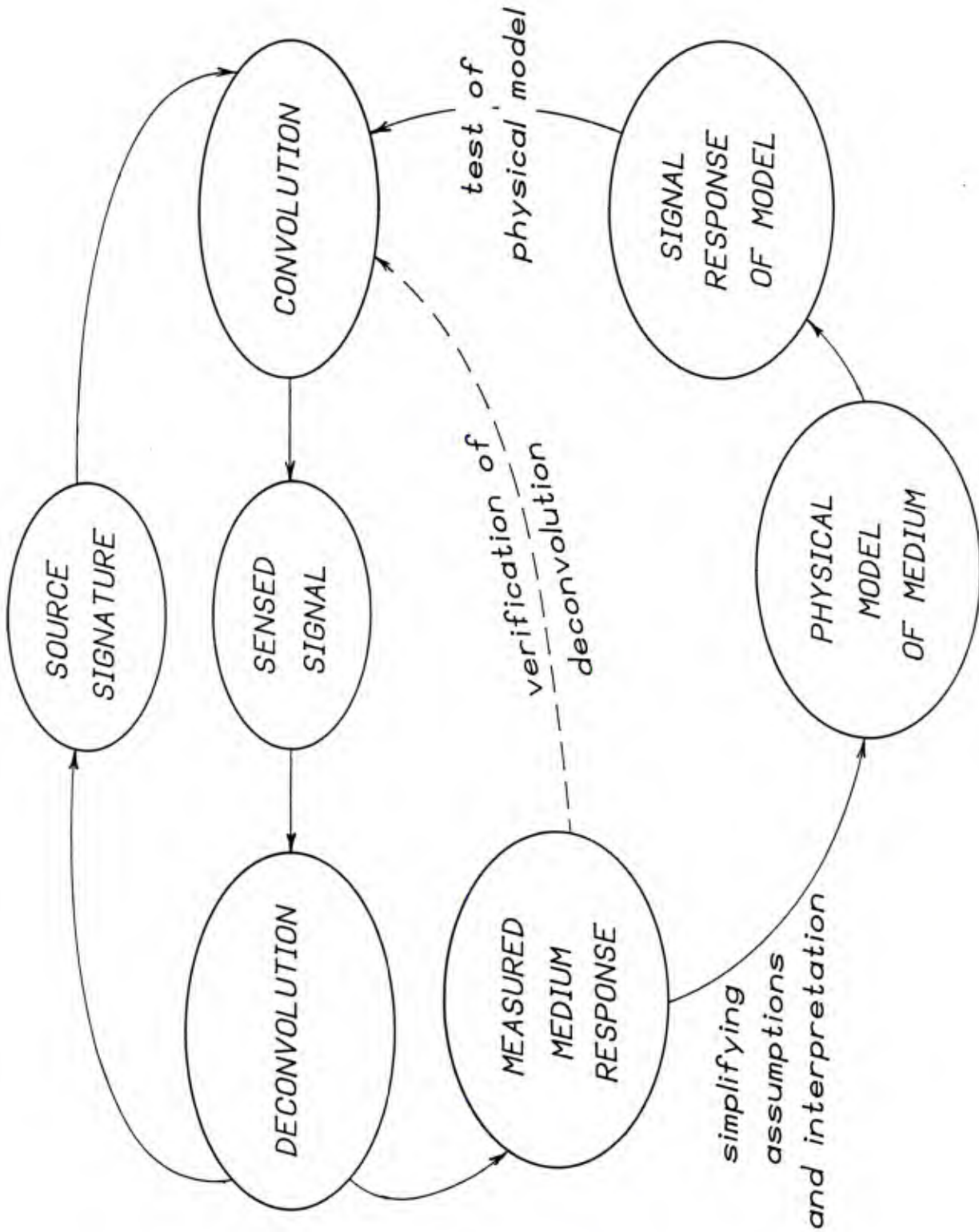


Figure 3. Complete system for ocean floor impulse response measurement and validation.

THE PROBLEM

To better understand the motivation for enhancement of seismic measurements by explosives, we will briefly consider the process of measuring relevant acoustic parameters of the ocean floor. The most important of these quantities are compressional sound speed and density as functions of depth into the sediment. At low frequency (less than 100 Hz) or in shallow water (a few wavelengths or less), the shear sound speed and attenuation may also become important.

The depth to which these quantities must be known depends on the geometry of the process to be modeled, the rate at which compressional or shear energy is dissipated in the sediment (the two attenuation parameters), and the acoustic frequency. Since viscous attenuation (constant loss per cycle) is generally assumed, the range of frequency to be covered by the model will set some limit on the depth to which we will need to know the properties.

Any experiment designed to measure these parameters must take into account the actual process to be modeled. If, for example, we are interested in low frequency detection of a single frequency source in deep water, we should try to make the measurement at a similar frequency and in deep water. In particular, the scale (in this case, the dimension-to-wavelength ratio) of the experiment should be close to the scale of the application. Attenuation in sediments is not linearly related to frequency over wide frequency ranges (as viscous attenuation theory applies) so the measurement frequency should be as close as possible to the application frequency for attenuation measurements. The experiment itself should not disturb the medium significantly and it should provide sufficient resolution in space so that the parameters can be determined as functions of depth and range.

In short, the measurement should be similar in, at least, scale and, perhaps, frequency to the system to be modeled and should probe the bottom sufficiently in depth and range without disturbance. Under these conditions, we must select a measurement method that will provide realistic estimates of the properties important for modeling underwater acoustic sensor performance.

Historically, sound speed and attenuation measurements have been made on thousands of samples of ocean sediment obtained by coring. For our purposes, these measurements are seriously deficient on at least two counts: first, the coring process produces substantial deformation of the sample thereby changing the physical properties; second, the measurements are generally made at several kilohertz so that the attenuation values are not applicable to low frequency investigations. Relatively little work has been done on scaled experiments and it would be difficult to construct a scale sedimentary column. In any case, attenuation values could not be measured reliably since scaling length downward means frequency must be increased (in order to preserve the length-to-wavelength ratio).

There are two major types of measurements made in the same environment as the operating system will be a part of. These are continuous wave (CW) and wideband, short-duration "shot" measurements. Although there is current interest in detection of broadband energy in the ocean, most ASW systems are designed for discrete frequency emissions from the target. In this sense, the CW measurements ought to be more realistic; however, the CW technique does have some disadvantages. As discussed below, the shot method can be considerably cheaper and faster than CW and, furthermore, the CW signal cannot be used to isolate different propagation paths (without beamforming). Therefore, the received CW signal is a single sine wave completely characterized by an amplitude and a phase and can only be used to measure the total propagation loss between a source and a receiver. If the water-borne path dominates, then very little information can be deduced about bottom properties.

One of the primary reasons for adopting the shot method for these ocean floor studies was that the entire experiment can be done from an airplane using sonobuoys and small explosive charges. In comparison with ship-based experiments, this technique is cheap and capable of surveying large areas quickly. The explosives - standard MK81 SUS - are reliable, repeatable, and result in a high signal-to-noise ratio at the receiver. Also, the bandwidth is high (roughly 50-10,000 Hz for a 2 lb charge at 800 ft) so that the potential time resolution, after enhancement, is good.

On the other hand, precise placement of the source and receiver is difficult, the source level at very low frequency (below 50 Hz) has not been accurately determined, the oscillating gas bubble makes enhancement difficult and, because of the large amount of energy released, the initial propagation of the pressure pulse is definitely nonlinear. This last problem can, in some instances, make application of the results to linear, CW propagation questionable.

In this report, we will consider only the enhancement of the received signal by removing the smearing effects of the explosion's gas bubble oscillation. This bubble is formed under very high pressure by the explosive's combustion products and it expands until the gas/water momentum is checked by the surrounding fluid pressure. The bubble has, at this point, over-expanded, so it is forced back in towards its center. Since the gases are quite elastic and the flow of the surrounding water is spherically symmetric, this oscillation continues for a number of periods until the energy is essentially dissipated and an equilibrium is reached between the gas pressure and the static fluid pressure. Typically, four to six cycles are visible on the received waveform of such an explosion. Without eliminating these oscillations, only gross properties of the bottom can be studied. If the oscillations can be removed, the time resolution of the received signal can be greatly improved. Consequently, property estimates along individual paths through the ocean floor can be made.

Before we discuss the process by which these received signals are enhanced, let us examine the formation of the received signal. While several points of view are possible, we will treat the problem as a system problem with some excitation (the explosion and bubble oscillation) and some response (the received waveform). The system is the ocean and its boundaries. One form of

excitation which we will not consider is a single-frequency sine wave. If we were to measure the output of the system for enough of these sine waves, each at a different frequency, we could completely determine the system response. This would be equivalent to measuring the received level from a sonobuoy for each setting of a variable-frequency CW source. In this manner, we could measure the frequency response of the system and then, given the spectrum of any arbitrary excitation, compute the response.

While the preceding method seems reasonable, it would in fact be difficult to do because of the need to sweep the source through a broad range of frequencies pausing long enough at each to achieve steady state, all the while maintaining the same experimental geometry. We can, on the other hand, probe the system at all frequencies in the band simultaneously if we choose an excitation waveform whose spectrum is uniform (that is, flat) across the band. The impulse is just such a waveform. Theoretically, the impulse has zero width and infinite amplitude so that the area enclosed is finite; however, for practical purposes, we will consider an approximate impulse that is very short duration and very high amplitude. With this impulse excitation, the received signal will have some characteristic shape called the impulse response: a fundamental system property.

To use this impulse response, we sample the excitation and then replace the sample points by weighted impulses so that the net area under the curve is conserved. As long as the system is linear, the response is just the sum of the impulse responses weighted and shifted in accordance with the original impulse sum. This weighting and shifting operation is called convolution and, in this instance, the time-domain waveform at the receiver is the convolution of the system's impulse response with the arbitrary excitation waveform. This convolution process occurs any time some physical system is excited. Each little "bit" (interval of time) of the excitation function acts as an impulse and the system responds accordingly. The output is the resultant of all of the impulse responses delayed in time to correspond with their respective bits of excitation.

This superposition of responses depends on the linearity of the system. In most cases, the systems with which we will work are linear, but remember that the explosion generates a large amplitude disturbance and until the amplitude decays sufficiently with range the propagation is nonlinear. If, for example, the explosion wavefront reflects from the ocean surface well before it becomes linear, the results may be quite different from those observed in a linear reflection. At this stage, we will have to be content with the linear theory but aware that the explosion may introduce errors into this assumption. Also, we should note that, while the signal enhancement process described herein is a nonlinear process, it does assume that the system on which it operates is linear.

In the next section, we will lay the theoretical foundation for a deconvolution process whereby the impulse response of the ocean system is extracted from the received signal. As we have seen, the received signal is formed by convolving the impulse response with the excitation waveform which, in our experiments, is an explosion's pressure pulse and bubble oscillation. If this

convolution can be undone, the impulse response and the source waveshape may be separated. Since the impulse response is the response of the ocean and ocean floor to an infinitely short pulse, we then would have a description of the propagation with potential for resolving individual propagation paths without the gross smearing caused by the gas bubble oscillations.

DECONVOLUTION THEORY

Convolution is a common phenomenon in physical problems in that a convolution occurs any time an external force is applied to a system. Real systems generally have some lag or delay in responding to an excitation and, perhaps, a resonant "ringing" or a decay that prolongs the response after removal of the excitation. Since this behavior is common, we will review some of the mathematical tools used to describe convolution before considering the methods for deconvolution.

As described in the previous section, the fundamental excitation is the impulse function and the fundamental system response is the impulse response. We will use the following notation to describe the excitation and response,

$$\delta(t) \rightarrow h(t).$$

The left-hand side is the excitation which, in this case, is the impulse (or delta) function. The right-hand side is the response (the impulse response in this example). The impulse function is defined as,

$$\begin{aligned} \delta(t) &= 1/dt \quad (dt \rightarrow 0) \quad \text{if } t = 0 \\ &= 0 \quad \quad \quad \text{if } t \neq 0 \end{aligned}$$

so that the following is true,

$$\int_{t_1}^{t_2} \delta(t-t_0) f(t) dt = f(t_0) \quad (t_1 < t_0 < t_2). \quad (1)$$

Thus, the impulse samples a function under integration.

A shift in time does not affect the system response, therefore,

$$\delta(t-\tau) \rightarrow h(t-\tau)$$

and, since the system is linear, we can form a superposition of these impulses as follows,

$$\sum_{n=0}^{\infty} f_n \delta(t-n\Delta t) \rightarrow \sum_{n=0}^{\infty} f_n h(t-n\Delta t).$$

For a continuous weighting function, the summation becomes an integration,

$$\int_0^{\infty} f(\tau) \delta(t-\tau) d\tau \rightarrow \int_0^{\infty} f(\tau) h(t-\tau) d\tau$$

but, because of the sampling property of the impulse, the left-hand side reduces so that

$$f(t) \rightarrow \int_0^{\infty} f(\tau) h(t-\tau) d\tau. \quad (2)$$

This equation expresses the system response mathematically. For an excitation $f(t)$, the system response is the convolution of that excitation with the system impulse response. If we know the impulse response, we can then calculate the system's response to any arbitrary excitation. (We have assumed above that the excitation starts no earlier than $t=0$. This is not necessary - just convenient.)

From this point, we will leave the time domain and concentrate on the frequency domain. Most of the literature that describes homomorphic deconvolution, the particular variety of deconvolution we are considering, uses the z-transform to establish the method's validity.^{3,4,5} Since we are ultimately going to use the fast Fourier transform (FFT) to convert from one domain to another, the discussion to follow will not explicitly mention the z-transform. Instead, the Fourier transform will be used and connection between the Fourier transform and the z-transform has been relegated to appendix A. Hopefully, this will make the process description more palatable to the non-specialist.

Take the Fourier transform of the convolution integral, equation (2),

$$G(\omega) = \iint_0^{\infty} f(\tau) h(t-\tau) e^{-i\omega t} dt d\tau$$

Next, expand the exponential factor,

$$G(\omega) = \iint_0^{\infty} f(\tau) e^{-i\omega t} h(t-\tau) e^{-i\omega(t-\tau)} dt d\tau$$

and make change of variables as follows,

$$\begin{aligned} t' &= t - \tau \\ dt' &= dt \end{aligned}$$

so that,

$$\begin{aligned} G(\omega) &= \int_0^{\infty} f(\tau) e^{-i\omega \tau} d\tau \int_0^{\infty} h(t') e^{-i\omega t'} dt' \\ &= F(\omega) H(\omega) \end{aligned}$$

where $F(\omega)$ = Fourier transform of $f(t)$

$H(\omega)$ = Fourier transform of $h(t)$.

Hence, a convolution of two time functions is equivalent to the product of their spectra. In symbolic notation, this property can be stated as follows,

$$\begin{aligned} F[f*h] &= F[f(t)] F[h(t)] \\ &= F(\omega) H(\omega) \end{aligned} \quad (3)$$

where $F []$ = Fourier transform
 $*$ = convolution

As a consequence of equation (3), we can now compute the system output (in the frequency domain) by multiplying the spectrum of the excitation by the spectrum of the impulse response. In addition, we could deconvolve by division: if we want to extract the impulse response of the system, we can divide the spectrum of the system output by the spectrum of the excitation and the result will be the spectrum of the impulse response.

The success of this type of deconvolution depends, however, on two factors. First, the excitation spectrum must be accurately known, and in these airborne seismic measurements the excitation is rarely directly measurable. Second, the excitation spectrum can never be zero (or, for that matter, small) at any frequency in the band of interest since the resultant response would be undefined (or extremely large) at these frequencies. This problem is usually circumvented by adding some noise to the excitation to fill in spectral nulls.

This deconvolution by division is known as inverse filtering and much work has been done in this area. If the source waveshape is well known, this is probably one of the best methods for computing impulse response; however, we will not say much more about inverse filtering.

Homomorphic deconvolution promises to be considerably more flexible, particularly in the case of a very complicated system such as the ocean and ocean floor. As we will see, it should be possible to isolate not only the impulse response but also certain parts of the impulse response or even the excitation itself. It is this processing flexibility that makes the homomorphic technique attractive.

Linear filtering of signals is a very useful and flexible procedure for noise removal or signal shaping because the filtering can be done in the frequency domain. If we consider a signal to be a superposition (that is, a summation) of sine waves of different frequencies and amplitudes, these component waves can be selectively removed or amplified in the frequency domain. The basis for homomorphic deconvolution is the location of a domain in which convolution becomes addition. Once this domain is found, the highly-developed techniques of linear filtering can be applied to separate or modify the various components. Thus, homomorphic deconvolution involves a nonlinear transformation of the convolved signal to reduce the convolutions to summations and subsequent linear filtering to extract the desired information.

We have already reduced convolution to multiplication by means of the Fourier transform. If we can reduce the multiplication to addition, we will in principle, have developed the required process. The logarithm function

reduces multiplication to addition but the numbers on which we must operate (the spectrum values) are complex. Hence, we must define a complex logarithm such that,

$$\text{Ln} (XY) = \text{Log}(X) + \text{Log}(Y)$$

where

$$X, Y = \text{complex numbers.}$$

This condition will be satisfied if,

$$\text{Ln} (X) = \ln|X| + i \arg(X) \quad (4)$$

or, if

$$X = |x| e^{i\phi} \quad (5)$$

then,

$$\text{Ln} (X) = \ln(x) + i\phi$$

where

\ln = natural logarithm
 \arg = argument function
 $| |$ = absolute value.

Another equivalent definition is possible by generalizing the definition of the natural logarithm,

$$\ln (x) = \int_1^x \frac{dx}{x}$$

where x is real. If we substitute a complex z for x and change the integration to a contour integration, we have,

$$\text{Ln} (z) = \int_1^z \frac{dz}{z} \quad (6)$$

The integral form of equation (6) is not a very practical definition but it serves to illustrate a problem in determining the imaginary part of the complex logarithm. According to equation (4), the imaginary part is the phase of the complex number; however, in the exponential notation of equation (5) this phase is ambiguous. Any integer multiple of 2π can be added to the phase factor ϕ in equation (5) without changing the value of the complex number. This addition will change the logarithm though. Equation (6) is a contour integral and the integral has only one pole at $z=0$. Therefore, any contour will produce the same answer as long as the contours all encircle the origin in the same way. The addition of multiples of 2π to the phase of the complex number is equivalent to circling the origin that same number of times and the resultant value is a function of the number of origin "orbits".

While we are generally accustomed to reducing the phase of a complex number to its principal value, we must not do so if we intend to use the complex logarithm. If the generating function for z is a continuous function, the phase relationship of nearby points can be determined by examining many closely-spaced points in between and, in this manner, the absolute (i.e., non-principal value) phase can be established.

Our problem is complicated by the fact that we operate on sampled signals and sampled output from FFT routines. In this case, the phase can change so much from one point to the next that the absolute phase is lost. One might naively believe that this could not happen since the signals are properly sampled to prevent aliasing but this sampling criterion (the Nyquist rate) is based on linear theory and the phase is a nonlinear function of the spectrum value. (The phase is the arc-tangent of the ratio of the imaginary part to the real part.) While the sampling may be adequate to define linear functions of the signal, there is no reason to expect that nonlinear functions are adequately sampled also. In fact, the phase is frequently severely under-sampled in the signals considered by this study. The aliasing that results⁴ from this under-sampling is discussed in terms of the z -transform by Ulrych⁴ and Stoffa.⁵

This then is the principal problem with homomorphic deconvolution. If the absolute phase can be correctly established at every one of the sample points of the spectrum, the deconvolution process can be continued. We will defer the discussion of how this can be done until the next section and continue with the theoretical development as if the absolute phase problem has already been solved.

Having successfully calculated the complex logarithm of each point in the spectrum, we have effected a transformation into the log-spectral domain. In this domain, the respective components of signals that were convolved in the time domain are summed. Since the combination of components is now linear, we can draw upon an extensive set of linear filtering techniques. Usually these techniques are applied to time signals by first transforming the signals into the frequency domain where the additive components (the constituent sine waves) become separated along the frequency scale. In this same way, we will transform the log-spectrum into another domain in which the additive components (which were convolutional components in the time domain) become separated.

Application of the Fourier transform to the log-spectrum generates a function called the complex cepstrum. Originally, the real logarithm of the magnitude spectrum was used to generate the cepstrum thereby losing the phase information. This was still a useful device for some applications but, without the phase information, deconvolution can only be done in some very special cases (which are discussed below). With this early work⁶ came a lexicon of new terms describing the various attributes of the cepstrum; however, most of these words serve only to confuse the real workings of the process so we will retain only the word cepstrum.

Actually, the important domain is the log-spectral domain because it is here that the convoluted time functions first become linear. The cepstrum is valuable primarily as an aid to filtering; in fact, the filtering, once developed, can be applied directly to the log-spectrum.

At this point, let us consider an example in order to clarify the relationship between the log-spectrum, the cepstrum, and the time function. The bubble oscillations of an underwater explosion affect the spectrum by introducing a definite oscillation (periodic along the frequency scale) of the spectrum magnitude. A Fourier transform of this magnitude spectrum (or the log-spectrum) should show a discrete peak at a time corresponding to the rapidity of the oscillation in the frequency domain. This peak does, in fact, appear in the cepstrum and the time (the scale of the cepstrum is time) corresponds to the period of the bubble oscillation. In general, the cepstrum scale is related to the time between repetitions of an event in the time series (such as echoes or multiple paths of propagation).

Another more specific example is helpful at this state. Consider a system whose response is a series of echoes; the impulse response for such a system is a sequence of delta functions,

$$h(t) = \sum_{i=0}^m a_i \delta(t-t_i). \quad (7)$$

The response for an arbitrary excitation $f(t)$ is then a sequence of weighted and delayed replicas of $f(t)$,

$$\begin{aligned} g(t) &= f * h \\ &= \sum_{i=0}^m a_i \int f(t-r) \delta(r-t_i) dr \\ &= \sum_{i=0}^m a_i f(t-t_i) \end{aligned}$$

where $g(t)$ = system output.

Furthermore, the frequency response, equation (3), is,

$$G(\omega) = F(\omega) \int_0^{\infty} \sum_{i=0}^m a_i \delta(t-t_i) e^{-i\omega t} dt$$

or

$$G(\omega) = F(\omega) \sum_{i=0}^m a_i e^{-i\omega t_i}$$

and the log-spectrum is,

$$\text{Log } [G(\omega)] = \text{Log } [F(\omega)] + \text{Log } \left[\sum_{i=0}^m a_i e^{-i\omega t_i} \right].$$

More specifically, consider one arrival and a phase-inverted echo delayed by 2τ seconds so that,

$$\begin{aligned} \sum_{i=0}^m a_i e^{-i\omega t_i} &= 1 - e^{-i\omega 2\tau} \\ &= 2e^{-i(\omega\tau - \frac{\pi}{2})} \sin(\omega\tau) \end{aligned}$$

and,

$$\begin{aligned} \text{Log } [G(\omega)] = & \text{Log } [F(\omega)] + \ln 2 \\ & -i \left(\omega\tau - \frac{\pi}{2} \right) + \ln [\sin (\omega\tau)]. \end{aligned} \quad (8)$$

The last two terms on the right-hand side deserve some comment. The last term is periodic in ω and will, therefore, lead to a peak in the cepstrum at τ seconds which is proportional to the echo time or, in other words, the repetition rate of the basic excitation waveform. The next to last term in equation (8) is linear in ω and can, therefore, lead to very large values in comparison with the last term. This could easily swamp the more important final terms. Fortunately, this term can be eliminated merely by shifting the waveform $g(t)$ in time (by τ seconds in this case) so that the two impulses of the $h(t)$ function are centered around $t=0$. This term, the linear phase ramp term, is generally present in the log-spectrum but it can always be eliminated by shifting the time series.

There is another aspect of the complex logarithm that causes a considerable amount of trouble and that is its value for very small arguments. In real signals, we are normally not troubled by poles in the spectrum but nulls or regions of low level are common. Through the logarithm operation, zero points in the spectrum become poles. Thus, any regions of very low level in the spectrum will be troublesome in the course of transformation to the log-spectrum.

To visualize the relationship of zeros in the spectrum to the transform process, we will generalize the Fourier transform. (Appendix A describes some of the relationships between the Fourier transform and several other transforms.) The Laplace transform is basically a generalized Fourier transform and the z-transform is a generalized discrete Fourier transform (DFT). Since we will eventually be using the FFT (an efficient computer algorithm for computing the DFT) to perform the necessary transformations, we will present the following discussion in terms of the z-transform. Usually, the z-transform is defined for sequences or sampled functions rather than for continuous functions, but, for our purposes, we will extend the definition to continuous functions.

Let us define our z-transform as follows (compare to equation (A-4) in appendix A),

$$G(z) = \int_0^{\infty} F(\omega) z^{\omega} d\omega$$

which reduces to the Fourier transform if the complex variable z is replaced by $e^{i\omega}$. Notice that the transform is written in terms of ω instead of z since we will forward transform the log-spectrum to enter the cepstrum domain.

Figure 4 shows the z-plane and the circular contour (a unit-radius circle centered on the origin) followed in the special case of the Fourier transform. As real ω increases, the integration progresses around this circle in the

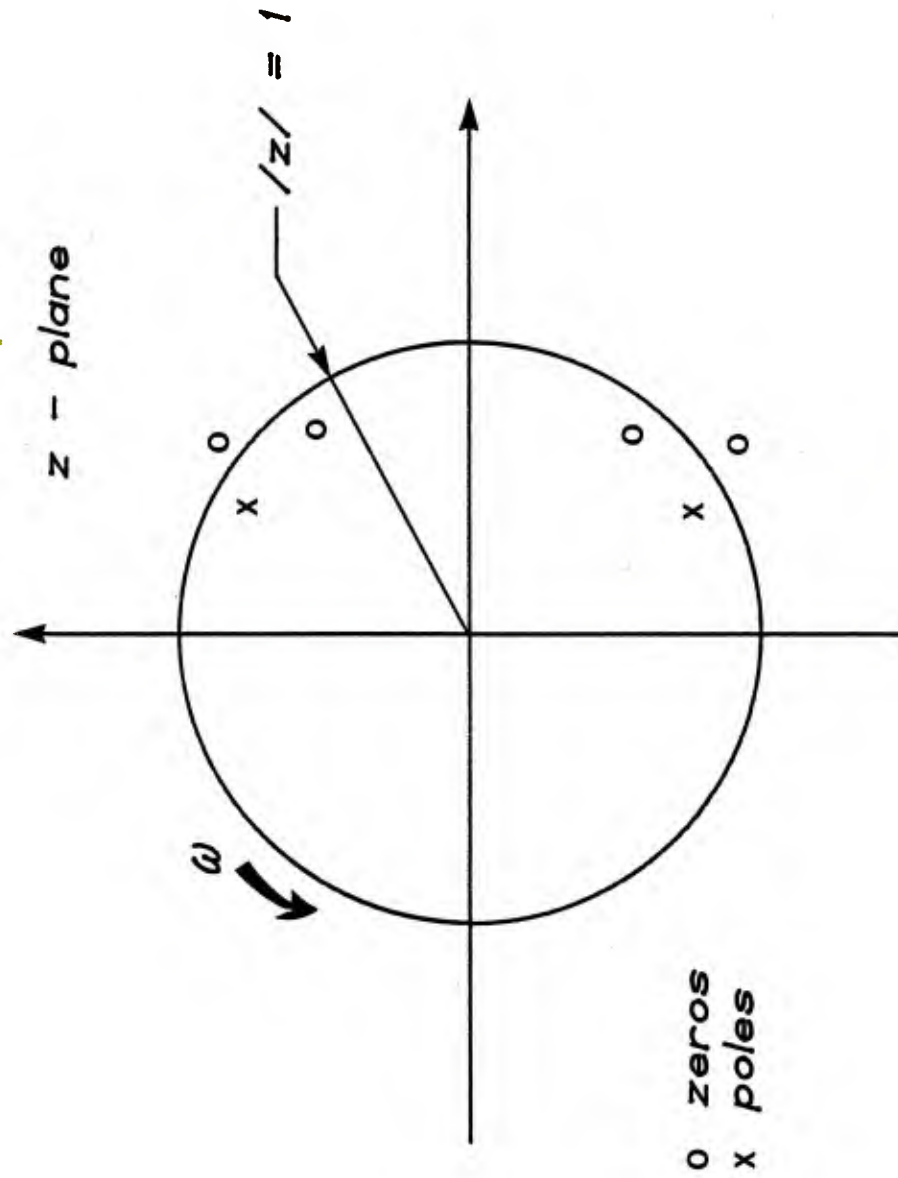


Figure 4. Fourier transform path in complex z -plane.

counter-clockwise direction. In order to evaluate the Fourier transform, we only need to know the values of the spectrum along this circular path. It is, however, useful to examine the spectrum in the z -plane near this path as its behavior near the path affects its value on the path. For example, we recognize the difficulty involved when a zero of the spectrum falls on the Fourier transform path: the complex logarithm becomes indeterminate. If a zero is near the path, the trouble is not as obvious but a spectral minimum will result accompanied by a rapid phase change.

To examine the influence of zeros close to the unit circle in the z -plane, let us consider a spectrum defined by a single zero and no poles,

$$F_o(z) = A_o(z - z_o)$$

where $F_o(e^{j\omega}) = F_o(z)$ for z on the unit circle. This situation is pictured in figure 5 along with two vectors corresponding to the difference $(z - z_o)$ for two values of z on the unit circle. As the frequency increases from ω_1 to ω_2 , the length of the vector from z_o to z decreases to a minimum at the point of closest-approach of the circle to z_o and then increases again. For the same progression of frequency, the phase continually decreases (clockwise vector rotation) slowly at first, then rapidly past the closest-approach point, then slowly again. These changes are illustrated in figure 6. If the zero is inside the unit circle, the variations are similar but the phase increases with increasing frequency.

Poles will appear in the z -plane if there is any trapped propagation in the ocean floor (that is, ducting by sediment layering or gradients) or one of several types of boundary waves. These effects are discussed in detail in the companion volume¹ to this report; but, in short, poles affect the phase in a manner similar to zeros. When a pole is near the unit circle the phase will also change rapidly as the contour passes by the pole. In the case of poles, we also know from stability theory that for physical (naturally stable) system, the poles will be inside the unit circle and so we can predict what direction the induced phase change will be. Since the factor $(z - z_o)$ is in the denominator for a simple pole, the direction of the phase change is opposite to that associated with a zero. Hence, the phase will decrease rapidly near a pole just inside the unit circle.

Since, in practice, the spectrum is sampled, there often is not enough information to establish the direction of these very rapid phase changes. For a zero very close to the unit circle, the phase change is roughly $\pm\pi$ and this is the same magnitude as the ambiguity in phase of a complex number. (In other words, if we guess that the change was π when it actually was $-\pi$, the error is 2π which cannot be resolved from the complex number.) As we will see in the next section, these phase changes can be so rapid for real signals that even by increasing the sampling rate of the spectrum they are frequently misinterpreted. In short, the sampled spectrum itself is adequately determined but the presence of zeros (or poles) in the spectrum and the requirement for absolute phase make the log-spectrum very difficult to compute.

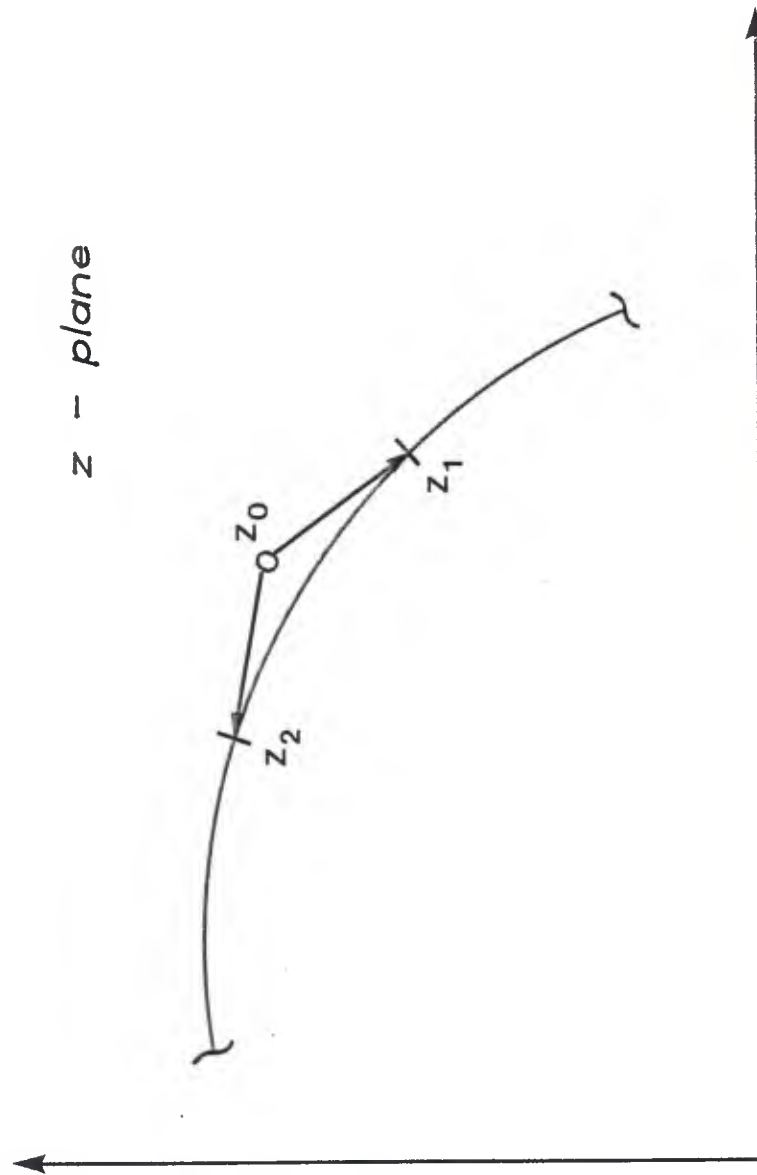


Figure 5. Construction of response for a single zero close to the Fourier transform path.

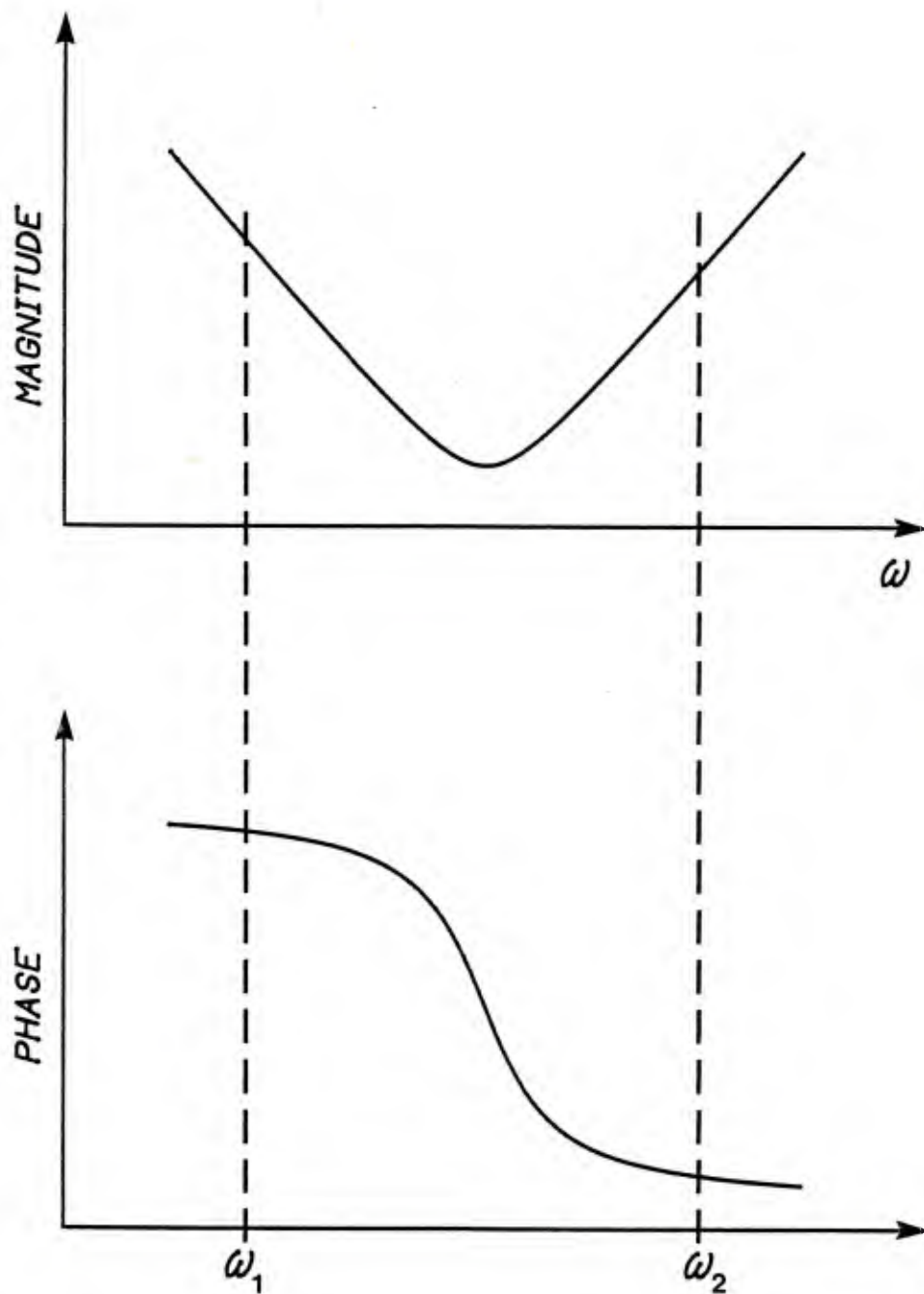


Figure 6. Magnitude and phase changes in spectrum for transform path that passes near a zero in the z-plane.

In general, the spectrum comprises a large number of zeros in the neighborhood of the unit circle and it is sometimes useful to move these zeros. For example, if there were several zeros very close to the unit circle, we could simplify the phase reconstruction if we could move them away from the circle. This is accomplished by exponentially weighting the original time series,⁷ as follows,

$$g(t) = f(t)\alpha^t. \quad (9)$$

The resultant spectrum is,

$$\begin{aligned} G(e^{i\omega}) &= \int_0^{\infty} f(t)\alpha^t e^{-i\omega t} dt \\ &= F(e^{i\omega}/\alpha). \end{aligned} \quad (10)$$

For α less than one, this is equivalent to sampling the spectrum along a circle outside of but concentric with the unit circle. From another point of view, this operation is equivalent to shrinking the spectrum symmetrically around the z -plane origin and still transforming along the unit circle. By using this exponential weighting, we can shift zeros that are close to the unit circle inside and farther away from the circle.

This operation of exponential weighting can help in the reconstruction of phase but it must be applied sparingly. The form of the factor α^t that multiplies the time series is such that, even for α close to one, the latter portions of the time series can be suppressed substantially. Fortunately, very small amounts of exponential weighting ($0.995 < \alpha < 1.00$) can significantly improve the reconstruction process.⁵

To conclude this discussion of deconvolution theory, we should mention the concept of minimum-phase.⁸ In general, both the real and the imaginary parts of the spectrum are needed to reconstruct the original time series, but, if the time series is causal (that is, zero for time less than zero), then the original series and, therefore, the imaginary part of the spectrum can be recreated from the real part of the spectrum. Thus, the real and imaginary parts of the spectrum of a causal time signal are related. In particular, the imaginary part is the Hilbert transform of the real part. This transform is very simple to apply: the inverse Fourier transform of the spectrum with only the real part nonzero is taken, the resulting time series is set to zero for all time less than zero, and then the forward Fourier transform is taken. The result is a spectrum with the real part unchanged and the appropriate imaginary part.

This same concept can be extended to the log-spectrum. In this case, the real part (the log-magnitude of the spectrum) is well-defined and single-valued. It would be convenient if we could extract the imaginary part (the phase of the spectrum) from the real part. This is possible if the cepstrum is zero for time less than zero. This is the condition for minimum-phase and, if it is true for a signal, the imaginary part of the log-spectrum can be calculated from the Hilbert transform of the log-magnitude spectrum. Under certain circumstances, we will be able to use this technique to eliminate the phase reconstruction problem; however, the minimum-phase condition is quite restrictive.

Oppenheim and Schafer⁸ show that if all of the poles and zeros of a spectrum are inside the unit circle, then the signal is minimum-phase. (Only the poles are required to be inside the circle for a stable signal.) As we have seen, we can force all of the zeros inside the unit circle by sufficient exponential weighting; however, this can lead to obliteration of most of the time series. Hence, we cannot indiscriminately force a signal to be minimum-phase and expect to get meaningful results. If a single convolutional component of the signal is almost minimum-phase and the other components can be averaged out by summing many log-spectra, we can take advantage of a small amount of exponential weighting and the Hilbert transform to extract the nearly minimum-phase component. We will outline an application for this procedure in the next section.

Before leaving the subject of minimum-phase, consider the type of signal that is minimum phase. Since we know that exponential weighting, in effect, moves zeros (and poles) toward the origin (for $\alpha < 1$), and we know that a signal is minimum-phase if all of its poles and zeros are within the unit circle, we would expect that a time series that, on the average, decays exponentially would be minimum-phase. This is generally true. The waveform of an explosion with its high-level shock front and decreasing amplitude bubble pulses is nearly minimum-phase. A series of reflections of decreasing amplitude from a normal incidence reflection from a layered medium would be almost minimum-phase. On the other hand, a near-grazing reflection from the ocean floor with refracted arrivals appearing later and stronger than directly reflected arrivals would not be minimum-phase. This intuitive view of minimum-phase is of some value in deciding on the method for phase reconstruction, but it certainly should not be accepted as proof of the nature of any signal. Since the process described in this report is nonlinear, each type of signal will have to be individually examined for peculiarities. In the nonlinear world, generalizations are dangerous.

APPLIED HOMOMORPHIC DECONVOLUTION

In this section, we will consider the problems and techniques associated with the application of deconvolution theory to real signals. These techniques tend to be application-dependent and so some modifications will undoubtedly be necessary in order for these processes to work on types of signals other than those considered herein. We have concentrated on deconvolution of seismic measurements of the ocean floor made with explosives and sonobuoys over wide ranges of incident angle. As a result, the following discussion will be tailored toward these types of signals; however, the principles involved should help the designer of homomorphic processors for other types of convolved signals.

Before we describe the mechanics of a homomorphic deconvolution process, let us review the major obstacles. For our purposes, the desired end product of deconvolution is the system impulse response (that is the received signal for a sharp excitation pulse after reflection from the ocean floor). This response

is the system output with all frequencies in the band of interest excited. Unfortunately, the explosion does not excite all frequencies uniformly. Furthermore, filtering in the data acquisition system eliminates still more of the desired information. The source waveshape spectrum rolls off quickly below the fundamental frequency of the bubble oscillation (approximately 50 Hz for a 2.2 lb TNT charge at 800 ft) and above that there are many nulls in the spectrum. In spite of the very high signal-to-noise ratio signal produced by the explosion, the noise in these nulls can dominate. This information is lost in any kind of deconvolution process.

Inadequate sampling of the spectrum creates another problem unique to homomorphic deconvolution. While the signal is adequately sampled for linear operations, the phase spectrum can be grossly undersampled. Consider the sampled spectrum of an actual measurement (with noise) of which four adjacent spectrum points are plotted in figure 7. This is a properly sampled signal according to Nyquist's criterion but there is no clear connection from one point to the next. Although it becomes expensive quickly, we can increase the sampling of the spectrum by adding zeros to the end of the time series prior to transforming. For example, if the original time series is 256 points long and 256 zero points are appended, the resulting spectrum will still cover the same frequency range but will be sampled twice as densely.

Figure 8 shows the same four points as figure 7 but with a curve superimposed by increasing the spectral sampling by a factor of 16. Now the sequence of phase (and magnitude) from point to point is clear and quite unexpected. The phase change from one point to the next is very large (the order of 2π) and at one point the curve passes so close to the origin that this large increase in resolution was necessary for establishing the path. If we pass the origin on the wrong side, we permanently accumulate a 2π error in the phase of all succeeding points. This close pass is the result of a zero very near the unit circle in the z-plane. By the direction of the phase change (a decrease), we know that this zero must be outside the unit circle and we cannot, therefore, be dealing with a minimum-phase process.

Some attempts have been made to reconstruct phase by integrating the phase derivative.⁵ This sounds round-about, but the derivative of phase with respect to frequency is single-valued, whereas the phase itself is not. The phase is,

$$\phi = \tan^{-1} (y/x) \quad (11)$$

where

$G = x + iy$, the complex spectrum point,

and this can only be computed as a principal value without additional information about the absolute phase. On the other hand, the derivative,

$$\begin{aligned} \frac{d\phi}{d\omega} &= \frac{1}{1 + (y/x)^2} \frac{d}{d\omega} \left(\frac{y}{x} \right) \\ &= \frac{xy' - yx'}{x^2 + y^2} \end{aligned}$$

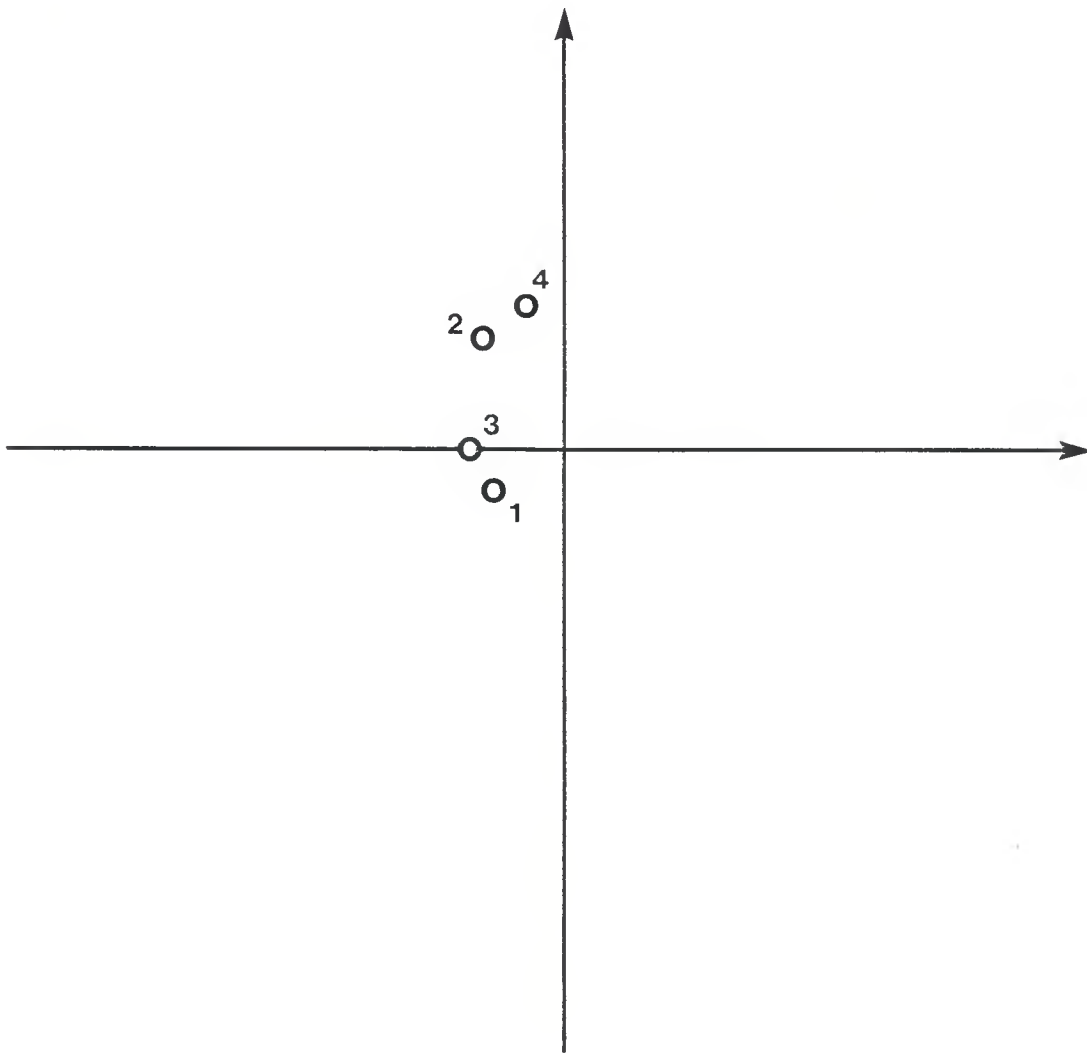


Figure 7. Four adjacent spectrum points of a properly-sampled real signal plotted in the complex spectrum plane.

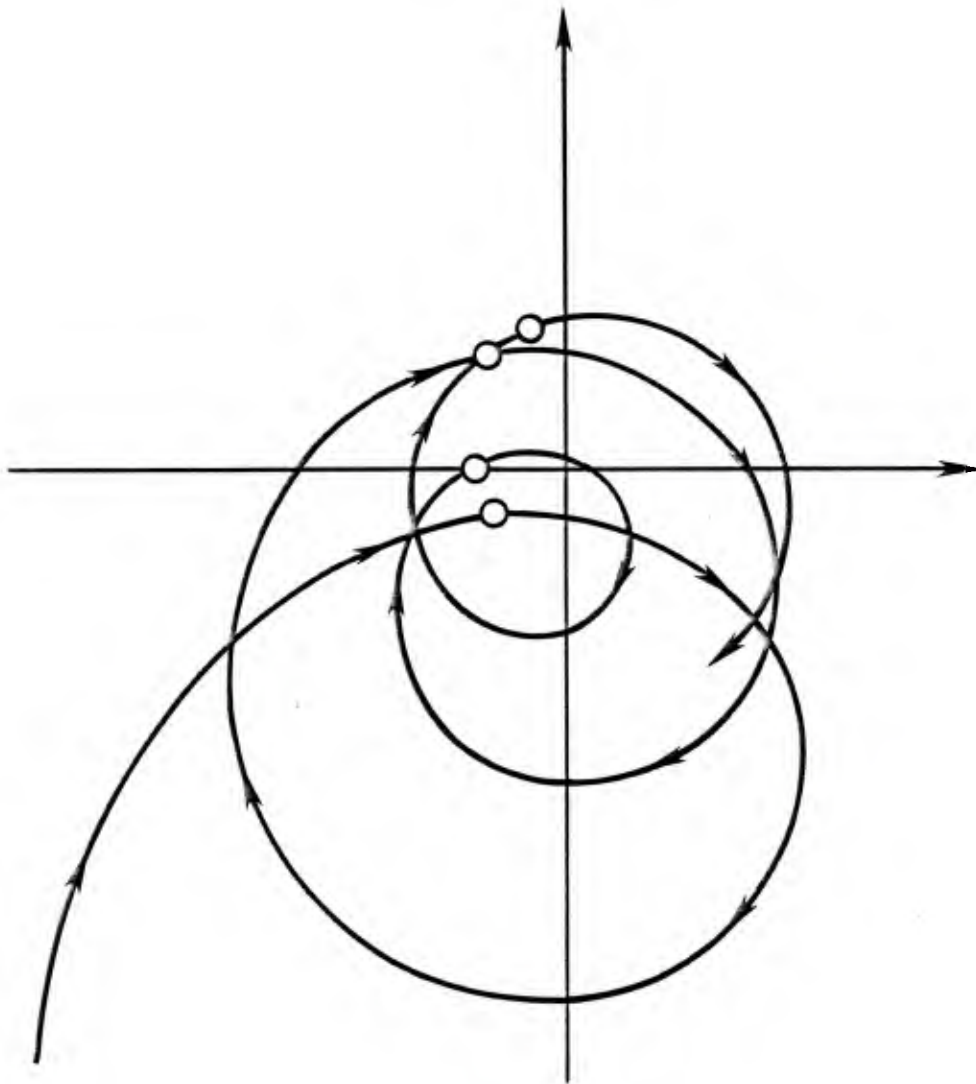


Figure 8. Actual spectrum progression between the four points of figure 7.

where the primes indicate differentiation with respect to ω , is single-valued. Given a suitable starting value, this expression can be integrated to give absolute phase. Unfortunately, this method is extremely susceptible to under-sampling. The phase derivative curve and our four sample points are shown in figure 9. Some of the peaks in the derivative curve are missed completely and even when one is hit the behavior of the curve is very poorly represented. Thus, the integration produces erroneous values. Tribolet⁹ attempted to solve this problem with an adaptive scheme that compares the integrated phase's principal value with the value computed by the arc-tangent. This procedure is somewhat more reliable, but when a sample point lands on one of the phase derivative peaks the phase can be off by one or more complete cycles. This happened frequently enough to abandon the phase derivative method.

Since the spectrum is undersampled, any reconstruction method must first increase the sampling density in the frequency domain. Large increases in resolution by zero-filling the time series are not economical, but this is a good technique to use in moderation. The smooth trajectory of the curve in figure 8 suggests that a curve-fit might be successfully applied to a moderate sampling increase. First, the spectrum sampling rate is increased by a factor of eight. Then these points are fit with a series of complex cubic splines based on sets of six adjacent points. Several curve-fits were evaluated and this seemed to work the best (see figure 10); however, even the six-point spline sometimes passed on the wrong side of the origin.

At this point, a decision must be made as to how to proceed. If we are content that each point of the spectrum be considered valid (that is, not corrupted by noise), we can develop an algorithm (described below) to locate the point of closest-approach of the spectral trajectory to the origin. Having found the frequency corresponding to this point, we can calculate the DFT at that point and use that point to resolve the path ambiguity. Since there are only a limited number of very close passes in a typical signal, the discrete transform calculations are not expensive. This approach does presume that the spectrum value is a valid signal point even though it is of very low level. We would expect, at least in some cases, that noise would dominate in these spectral nulls and we do not want to permit noise to drive the reconstruction process.

A procedure which has not been tested adequately is based on a weighted curve-fit of the spectrum points. The spectrum is computed for increased resolution (four times is probably sufficient) and, as before, consecutive sets of the points are fit but in a least-square sense with the higher amplitude values weighted more than the lower values. Some type of bridging scheme like this has potential for enhancing phase reconstruction in the presence of noise.

The physics of the signal and the ocean medium may also be used to provide some constraints on the phase reconstruction process. Some preliminary studies of the phase progression in real systems have been summarized in the companion volume¹ to this report, and we have already discussed some of these results in connection with poles in the spectrum. We can, at least, tell beforehand which direction the phase change will be in near system resonances connected with

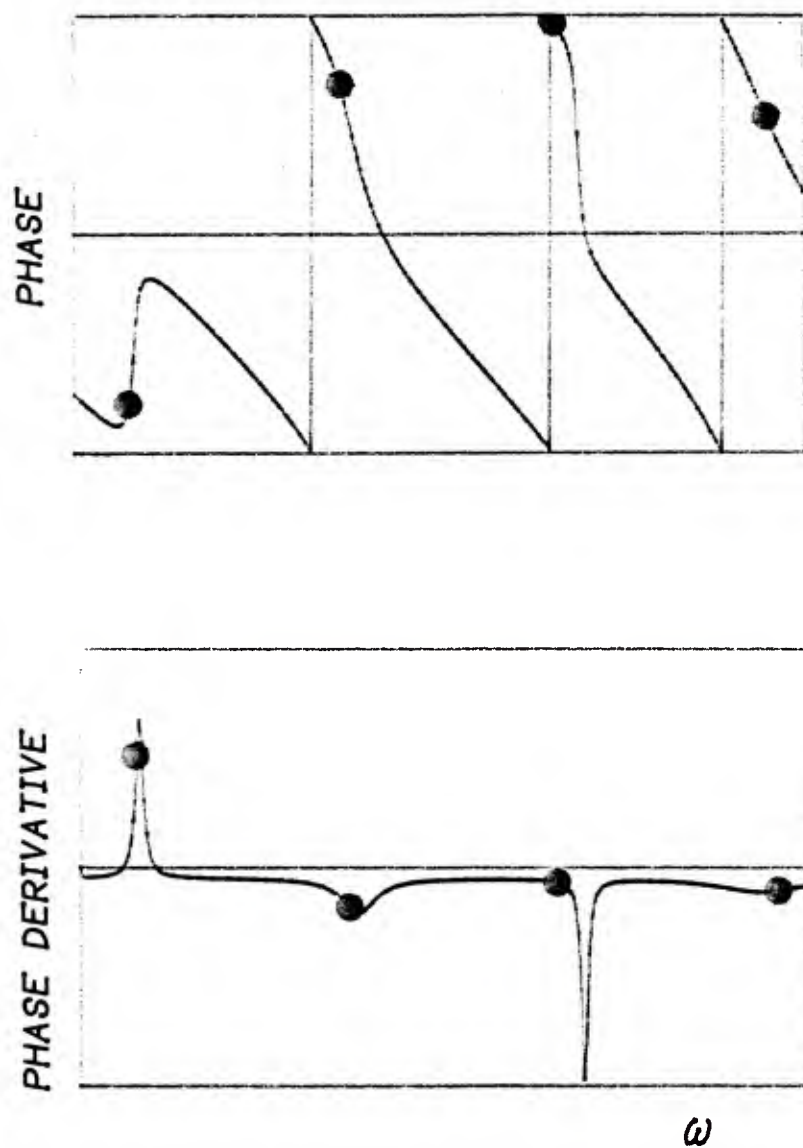


Figure 9. Sampling of phase and phase derivative for a typical real signal sampled at the Nyquist rate.

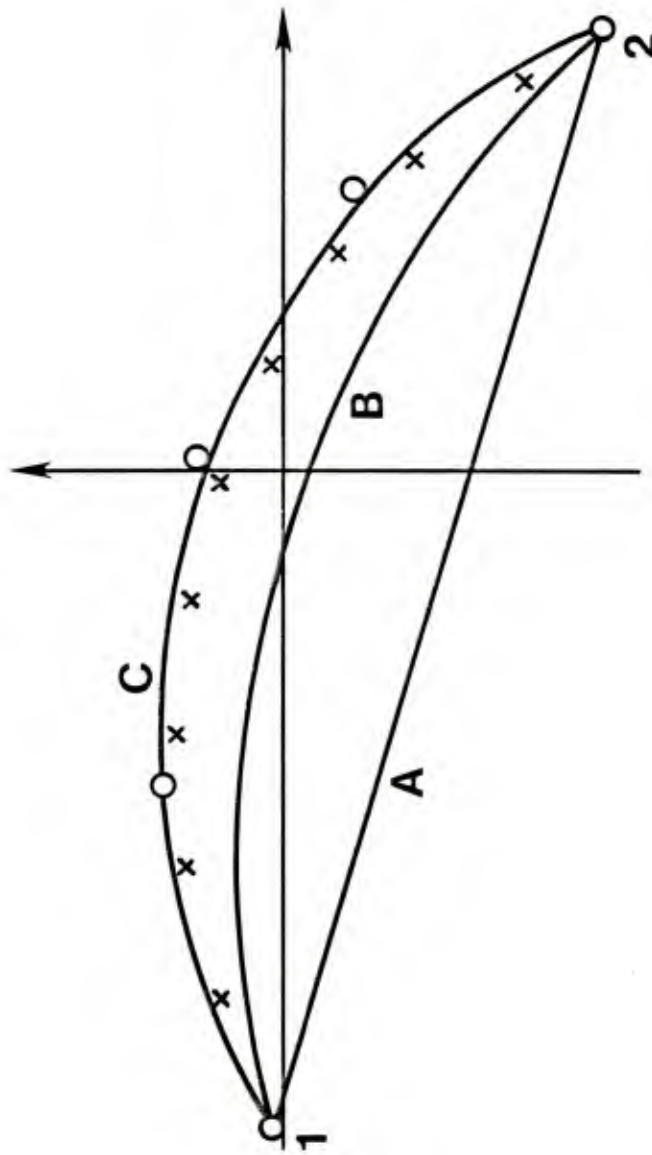


Figure 10. Various curve-fits of spectrum data: (A) straight line, (B) cubic curve fit to four points, (C) cubic spline fit to six points, (x) cubic spline fit to entire spectrum, (o) actual intermediate spectral points.

trapped or ducted propagation and boundary waves. Considerably more work needs to be done in this area in order to better understand the behavior of the phase spectrum of transient signals.

The technique used for most of the work presented here is the procedure based on locating the points of closest-approach and computing the DFT at this point. Several steps are involved here: first, close pass situations must be detected; next, the discrete transform must be evaluated; finally, the path route around the origin must be chosen based on this calculation.

In the interests of computational speed, a fairly crude (and conservative) scheme is used to detect potential close-pass situations. If the angular difference between successive points of the "oversampled" spectrum is less than 90° , we assume that the spectral trajectory between these points can be adequately represented by a straight line. By considering each of the two points as a vector emanating from the origin and taking the dot product of these vectors, the sign of the cosine of the included angle can be evaluated very rapidly since, if,

$$\bar{A} = (x_1, y_1)$$

$$\bar{B} = (x_2, y_2)$$

then

$$|\bar{A}|/|\bar{B}|\cos\phi = \bar{A} \cdot \bar{B} = x_1x_2 + y_1y_2 \quad (12)$$

where \bar{A} , \bar{B} are vectors in the spectrum-plane. If the dot product is positive, then the included angle ϕ must be less than 90° and we can proceed directly to detection of path direction.

On the other hand, if the included angle is greater than 90° , we fit the set of six adjacent points centered on the trouble spot with a complex spline (actually two real splines, one on the real parts of the points and one on the imaginary parts). A fast, bisection search is then performed to locate the closest-approach point and the DFT is computed at the corresponding frequency. The DFT need not, however, be taken on the entire time series, which is mostly zero (having been padded with zeros to increase resolution). Instead, we take the DFT of the unpadded time series and then adjust the phase of the spectrum point to reflect the shift of the original series within the field of zeros. The path direction is then determined from this intermediate point.

One important feature of the phase tracking procedure is that the actual path of the spectrum is immaterial as long as a count is maintained of the net number of orbits of the spectrum origin. With this count and the principal value of the phase at a point, the point's absolute phase can be determined merely by adding or subtracting a corresponding multiple of 2π . The count of origin orbits can be kept by counting the net number of crossings of the negative real axis in the counter-clockwise direction. This implies a branch at

$\pm\pi$ which is consistent with the principal value branch selected by the computer arc-tangent function. When it is necessary to compute a close-approach point, the crossing detection is done in two stages: from one spectrum point to the approach point and then from the approach point to the next spectrum point.

We have, in essence, solved the phase reconstruction problem for a sampled signal. In this implementation it is still possible for errors to occur, so as interactive test procedure is used. Since we must remove the linear (ramp) component of the phase change from one end of the spectrum to the other by shifting the time series, we can redo the phase reconstruction on this shifted series. The results should be the same after correcting for the linear phase shift induced by the time shift. The relationship between these two shifts can be found by taking the Fourier transform of a shifted time series,

$$\int_0^{\infty} f(t-t_0)e^{-i\omega t}dt = e^{i\omega t_0} F(\omega) \quad (13)$$

where

$F(\omega)$ = Fourier transform of $f(t)$.

The first spectrum point is the zero-frequency point so the absolute phase there is set to zero. The highest point in the spectrum ω_t , after the initial phase reconstruction, has some absolute phase ϕ_t that can be removed by time shifting according to equation (13) where

$$e^{i\omega_t t_0} \cdot e^{i\phi_t} = 1$$

or

$$t_0 = -\phi_t/\omega_t. \quad (14)$$

This will also affect every other point in the spectrum as follows,

$$F_s(\omega) = e^{-i\phi_t(\omega/\omega_t)} F(\omega) \quad (15)$$

where $F_s(\omega)$ = Fourier transform of the shifted time series. Thus, the phase shift is in the form of a ramp: zero at zero frequency, ϕ_t at the highest frequency, and linear with frequency in between.

If we had complete confidence in the initial phase reconstruction, we could remove the resulting phase ramp by a suitable time shift and proceed with the deconvolution. However, the process is not always error-free, so the reconstruction is repeated on the shifted time series. In addition to the usual test for reconstruction near zeros or poles, each new point is compared with each corresponding point in the previous pass to see if the phase has changed proportionately following equation (15). Any time a discrepancy is found, the spline fit and closest-approach calculations are performed to resolve the questionable point.

When this second phase reconstruction has been completed, the absolute phase of the last point in the spectrum should be zero (since the phase ramp was removed after the first pass). If not, the new ramp is removed and the reconstruction is performed again. In most cases, this is sufficient. If the endpoint phase is still not zero the procedure can be repeated, but this may be an indication that the signal cannot be adequately resolved by this technique.

If, on the other hand, the second or third reconstruction is successful (endpoint phase goes to zero), then the absolute phase values can be stored as the imaginary part of the log-spectrum. The real part is formed by the natural logarithm of the spectrum magnitude and this completes the calculation of the log-spectrum. Since generation of the log-spectrum is the key process in this method of deconvolution, a listing of a computer code for this operation is given in appendix B.

Most of this discussion so far has been centered on the phase reconstruction problem because this is the most difficult aspect of homomorphic deconvolution. The other processes cannot, however, be done carelessly. Proper conditioning of the signal prior to phase reconstruction is vital, and this conditioning will be discussed in some detail in the next section. In short, this preconditioning involves proper sampling, filtering, and exponential weighting.

Once the log-spectrum has been calculated, a standard FFT is applied to compute the complex cepstrum (unless the deconvolution filter has been designed to operate directly on the log-spectrum). Then the portion of the cepstrum, corresponding to the undesired part of the signal, is removed. Simply setting these points to zero is often sufficient. For example, if we want to eliminate the bubble oscillations of an explosive source, we zero a portion of the cepstrum around the bubble oscillation period (that is, the time between repetitions). We might also zero a small band of time corresponding to the repetition rate generated by unwanted multipath reflections.

Having isolated the desired portion of the cepstrum, we then perform the inverse FFT to return to the log-spectrum and then perform the complex exponential is computed as follows,

$$\exp(x+iy) = e^x e^{iy}$$

This function is completely unambiguous.

Finally, the inverse FFT is applied once again and the resulting time series is exponentially weighted by the inverse of whatever factor was used to weight the original time series. After shifting the series back to its original starting point in time, we have completely recovered the deconvolved signal. An example of the complete process is given in figure 11 where the source waveshape (A) is removed from a signal (A*B) with multiple arrivals. The received signal was synthetically generated by convolution of a replica of the explosion's bubble pulse and a three-path reflector series (B). While the

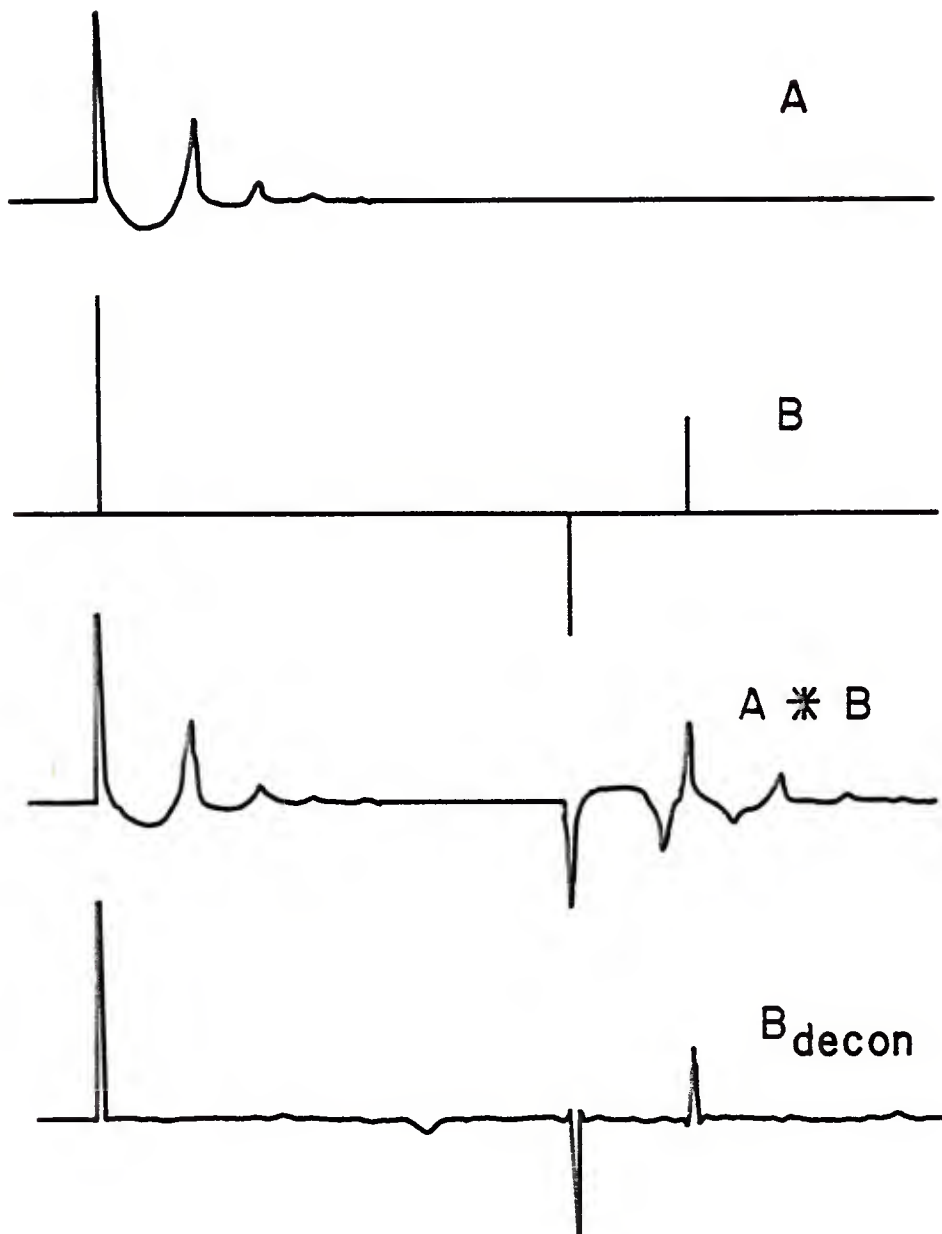


Figure 11. Example of homomorphic deconvolution of a received signal ($A*B$) made up of a source excitation (A) and a multipath medium response (B).

source waveform was known to construct the received waveform, this information was not used in the deconvolution. The deconvolution was performed by zeroing the cepstrum for all time at or below the bubble oscillation period.

Additive noise in the time domain can be tolerated up to a certain point without adversely affecting the process. Beyond this point, however, the phase reconstruction fails because the spectrum nulls and the attendant phase jumps become dominated by the characteristics of the noise. Hopefully, the previously mentioned null-bridging technique will reduce this problem. Until null-bridging is perfected, this type of deconvolution is probable restricted to high signal-to-noise signals. Fortunately, most of the ocean floor measurements with which we are concerned are high signal-to-noise, thanks to the high intensity sound generated by the explosive charges.

In the preceding section, the concept of minimum-phase was introduced. For reasonably deep, underwater explosions, the source waveshape is almost minimum-phase. This property can be exploited to extract the source waveform itself. Since the measurements on which we are operating are taken over a wide range of angles, the only component of the signal common to all received signals at a given site is the source waveshape. If we then add a large number of the log-spectra of these measurements, the components related to the ocean response will tend to cancel while the source components will build up. We can avoid the problem of phase reconstruction by sufficient exponential weighting to insure that the source waveform is minimum-phase and then by Hilbert transforming to generate the phase of the averaged log-spectrum.¹⁰ The ocean response need not be minimum-phase because these components are averaged out, each measurement having a different geometry and arrival structure.

After the averaged log-spectrum has been completed by Hilbert transformation of the averaged log-magnitude spectrum, the spectrum and corresponding time series are computed. Figure 12 shows an example of the isolation of the source waveform from 20 seismic measurements, each with a complicated arrival structure. The source waveshape extracted is very similar to the expected explosion waveshape.¹¹

Once the source waveshape is established in this way, one of the more conventional deconvolution processes (such as inverse filtering) may be used to obtain the ocean floor response. One practical point worth mentioning here is that the source waveform of each measurement may, in fact, be slightly different because the charge does not always detonate at the same depth. The depth of the explosion (along with the relatively constant charge weight) determines the period of the bubble oscillation. We can, however, measure this period quite accurately by the associated peak in the cepstrum and correct each measurement to the same depth by stretching or shrinking the time axis prior to averaging. The cepstrum computed from the log-magnitude with zero phase is adequate for measuring the bubble period.

It is also possible to perform this averaging deconvolution to extract the ocean floor response if the geometry is such that the reflection response is almost minimum-phase and the source waveshape can be forced to vary from

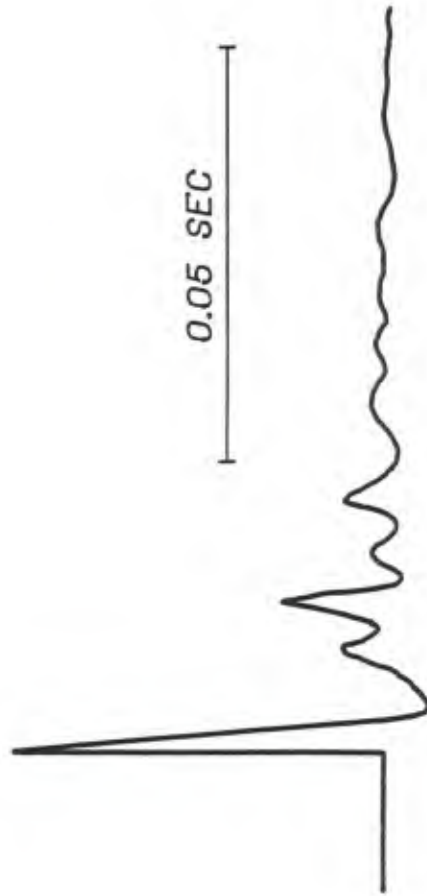


Figure 12. Reconstruction of explosive source waveform by log-spectral averaging.

measurement to measurement. A fairly high angle (i.e., near-vertical) measurement may satisfy the minimum-phase requirement with slight exponential weighting and several shots of varying depths and sizes could be used to vary the source waveshape.

Also, it should be possible to reduce the noise problem for any type of deconvolution by averaging spectra or log-spectra of a number of measurements with the same geometry and source waveshape. Neither of the last two proposals has been tried as each would require a new experimental design (probably in the form of a shipboard experiment), but they have enough promise to encourage their consideration in future experimentation.

SIGNAL CONDITIONING

As we have emphasized, the success of this signal process is dependent on the quality of the signal on which the process operates. Such general and powerful principles as superposition or Nyquist's sampling theorem have no equivalents in nonlinear processing. Each type of signal must be treated on its own merits and must be conditioned properly in order to insure a valid deconvolution. In this section, we will outline some of the ways in which signals should be conditioned as a part of homomorphic deconvolution.

First, let us review the basic problems with nonlinear deconvolution. In deconvolution, we are trying to reconstruct the response of a system at all frequencies (the impulse response) from the system output for an excitation that does not contain all frequencies. This means that, for those portions of the spectrum for which we have little signal, noise will corrupt the convolution. In addition, for operations with the log-spectrum, minimum-phase signals are ideal; however, we usually must deal with mixed-phase signals.

To avoid processing portions of the spectrum that are not well-excited by the source, we should filter and translate the original received signal for maximum energy across the remaining band. Remember that we are not free to select any band for the impulse response; the spectrum of the source determines what regions of the frequency response can be found. In general, we will have to low-pass filter to remove regions of high frequency noise and then translate to remove the poorly-excited frequency range below the explosion's bubble oscillation frequency. Some work has been done in breaking up the spectrum between these limits¹² so as to eliminate intervening spectral nulls resulting from the source, but we will not consider these techniques. For the present, it is sufficient to drop the high and low sides of the spectrum where the source energy is rolling off. The objective of this first step is to minimize the number and extent of low-level areas in the spectrum.

Next, the signal should be sampled as close to the Nyquist rate (that is, twice the frequency of the highest significant component of the signal) as possible. Undersampling, of course, will introduce aliasing. Oversampling may be just as bad, though, as oversampling effectively pushes the high frequency limit of the analysis up beyond the roll-off of significant energy

in the spectrum. This generates a region of low spectrum level that will be difficult to resolve during the phase reconstruction. Consequently, filtering of the signal should be done with a fairly sharp-edged filter so that aliasing can be avoided while still maintaining a near-optimum sampling rate.

In the type of signals considered in this report, there are generally a large number of zeros very close to the unit circle. Many of these result from the nearly-minimum-phase source waveform and they are all seen as large dips in the spectrum. The phase reconstruction can be simplified somewhat by a small amount of exponential weighting. As we have seen, this weighting moves the zeros toward the origin of the z-plane and, therefore, away from the unit circle. Since the amplitude of the time series decreases exponentially with time for this weighting, we must first shift the time series of the received signal toward the origin ($t=0$) so that the signal starts immediately on the time record. Also, the α in equation (9) should not be less than about 0.99 (and, of course, not greater than 1.00). Below this value, the time series is seriously attenuated toward the end of the record. As a result, it would be unusual if this limited magnitude of exponential weighting made the entire signal minimum-phase, but it may be enough to make the source component minimum-phase.

After the exponential weighting has been done, it is often helpful to shift the time series again. Since the phase ramp in the spectrum is undesirable and corresponds to a uniform shift or delay in the time series, we can reduce this ramp considerably by shifting the weighted time series so that it is approximately centered on $t=0$ (equal energy on both sides of $t=0$, for example). This will not, of course, completely eliminate the phase ramp, but it will simplify the first pass of the phase reconstruction.

In general, it is helpful to know as much as possible about the physics involved in a particular signal formation process. The physics of a process can indicate what convolutional components are likely to be present. In ocean floor seismic measurements, these components may include multipath effects, attenuation, and phase shifts. The medium-induced phase shifts may be particularly important as they can introduce signal distortion at ray turning points or at reflections from impedance discontinuities. Knowledge of the explosion's bubble-pulse formation and oscillation allows us to guess that this is close to a minimum-phase process and permits us to exploit some of the special properties of these processes.

CONCLUSIONS

One of the most important results of this study, aside from the development of the deconvolution process, is that the full homomorphic deconvolution with phase reconstruction is highly dependent on the quality and conditioning of the original signal. The process works well on signals that have a high signal-to-noise ratio, are strongly excited over most of the frequency range

of interest, and are properly sampled and weighted. While the phase reconstruction method described above is effective in many cases, sufficient degradation in the signal quality will eventually produce meaningless phase spectra. Consequently, applications of this deconvolution process will require careful checking of the quality of the input signals.

This is not to say that the process must be abandoned in the case of less strongly excited systems; however, further refinements may become necessary. The null-bridging technique may provide a means for resolving the phase over small regions of low signal level. In addition, physical constraints such as the phase change near poles of the spectrum or at ray turning points will be helpful in predetermining the phase progression. Development of these techniques will, however, require substantial testing and experience with real signals.

Extraction of almost-minimum-phase components by averaging deconvolution is a very effective process. In the measurements with which we are concerned, the only component that this is well-suited to is the source waveform. Information about the source waveform is, however, necessary in applying conventional deconvolution and so a hybrid process may be worthwhile. Such a process would isolate the source waveform by log-spectral averaging and then use this source waveform to develop an inverse filter. This would, of course, lose the flexibility of the fully homomorphic technique in that only the impulse response for the entire ocean system could be found.

While tests on small sections of experimental data have demonstrated at least a limited value in homomorphic deconvolution, much more experience must be gained in order to ascertain the extent of practical applications. This is true because the log-spectrum and the cepstrum are not well-known domains. Until the nature of signals in these domains becomes familiar enough to develop intuitive expectations that guide much of linear signal processing applications day-to-day, homomorphic deconvolution will remain a technique accessible to only a few specialists. Hopefully, much of this experience will be gained as this process is applied to the large volume of seismic measurements resident at NAVAIRDEVCON.

REFERENCES

1. Gabrielson, T.B., "Impulse response of the ocean floor: mathematical modeling," NADC-82254-30, 1982.
2. Dicus, R.L., "Synthetic deconvolution of explosive source acoustic signals in colored noise," NAVOCEANO TN-6130-3-76, Feb 1976.
3. Oppenheim, A.V., Schafer, R.W. and Stockham, T.G., "Nonlinear filtering of multiplied and convolved signals," Proc. IEEE 56, No. 8, pp. 1264-1291, Aug 1968.
4. Ulrych, T.J., "Application of homomorphic deconvolution to seismology," Geophysics 36, No. 4, pp. 650-660, Aug 1971.
5. Stoffa, P.L., Buhl, P. and Bryan, G.M., "The application of homomorphic deconvolution to shallow-water marine seismology - Part I: Models," Geophysics 39, No. 4, pp. 401-416, Aug 1974.
6. Bogert, B.P., Healy, M.J. and Tukey, J.W., "The quefrency alanalysis of time series for echoes," in Time Series Analysis, M. Rosenblatt, Ed., Wiley, NY, 1963.
7. Schafer, R.W., "Echo removal by discrete generalized linear filtering," MIT Research Laboratory of Electronics, TR-466, 1969. See references 4 and 5, also.
8. Oppenheim, A.V. and Schafer, R.W., Digital Signal Processing, Prentice-Hall, Englewood Cliffs, NJ, 1975.
9. Tribolet, J.M., "A new phase unwrapping algorithm," IEEE Trans. Acoustics, Speech and Sig. Proc. ASSP-25, No. 2, pp. 170-177, April 1977.
10. Stockham, T.J., Cannon, T.M., and Ingebretsen, R.B., "Blind deconvolution through digital signal processing," Proc. IEEE 63, pp. 678-692, 1975.
11. Wakeley, J., "Pressure-signature model for an underwater explosive charge," U.S. Navy J. Underwater Acoust. 27, No. 2, pp. 445-449, April 1977.
12. Tribolet, J.M., "Applications of short-time homomorphic signal analysis to seismic wavelet estimation," IEEE Trans. Acoustics, Speech and Sig. Proc. ASSP-26, No.4, pp. 343-353, Aug. 1978.

REPORT NO. NADC-82253-30

APPENDIX A
TRANSFORM RELATIONSHIPS

APPENDIX A

TRANSFORM RELATIONSHIPS

The integral transform pairs with which we are concerned in this report are the Fourier transform pair,

$$G(\omega) = \int_{-\infty}^{\infty} f(t)e^{-i\omega t} dt \quad (A-1)$$

$$f(t) = \frac{1}{2\pi} \int_{-\infty}^{\infty} G(\omega)e^{i\omega t} d\omega$$

and the Laplace transform pair,

$$F(s) = \int_0^{\infty} f(t)e^{-st} dt \quad (A-2)$$

$$f(t) = \frac{1}{2\pi i} \int_{\alpha-i\infty}^{\alpha+i\infty} F(s)e^{st} ds$$

which is essentially a generalized Fourier transform. For the special case of $s = i\omega$, the Laplace transform reduces to the Fourier transform as long as $f(t)$ is casual ($f(t) = 0$ for $t < 0$) and stable (which permits $\alpha = 0$).

Each of these integral transforms has a discrete equivalent that would be used on sampled series. The discrete equivalent of the Fourier transform is the discrete Fourier transform (DFT) given by the pair,

$$X(k) = \sum_{n=0}^{N-1} x(n)e^{-i2\pi kn/N} \quad (A-3)$$

$$x(n) = \frac{1}{N} \sum_{k=0}^{N-1} X(k)e^{i2\pi kn/N}$$

The discrete equivalent to the Laplace transform is written in terms of a new variable z which is equal to e^s . This transform is called the z -transform and the corresponding transform pair is,

$$X(z) = \sum_{n=-\infty}^{\infty} x(n)z^{-n} \quad (A-4)$$

$$x(n) = \frac{1}{2\pi i} \oint_C X(z)z^{n-1} dz$$

Notice that this transform is discrete in time ($t = n\Delta t$) but not in frequency; z is a continuous variable. The contour C of the inverse transform is any closed contour lying entirely in the region of convergence of the function $X(z)$.

The relationship between the various transforms can be seen by comparing figures A-1 and A-2. Figure A-1 shows the paths for the Fourier (F) and Laplace (L) inversion integrals in the z -plane. The z -transform inversion follows the same path as the Laplace inversion. In the case of the DFT, there would be N samples evenly spaced around the unit circle (the F path).

In the s -plane (figure A-2), the circular contours unwrap into the vertical lines F and L and, at the same time, the entire z -plane is replicated in the s -plane as an infinite series of horizontal layers. The interior of the unit circle maps into many horizontal bands to the left of the imaginary axis and the exterior of the circle maps into horizontal bands to the right. Classical stability theory says that there may be no poles in the right half of the s -plane; this corresponds to having all the poles inside the unit circle in the z -plane. For Fourier analysis, frequency starts at zero at the origin of the s -plane and increases vertically upwards. In the z -plane, spectral frequency is zero at $z = +1$ and increases counter-clockwise around the unit circle.

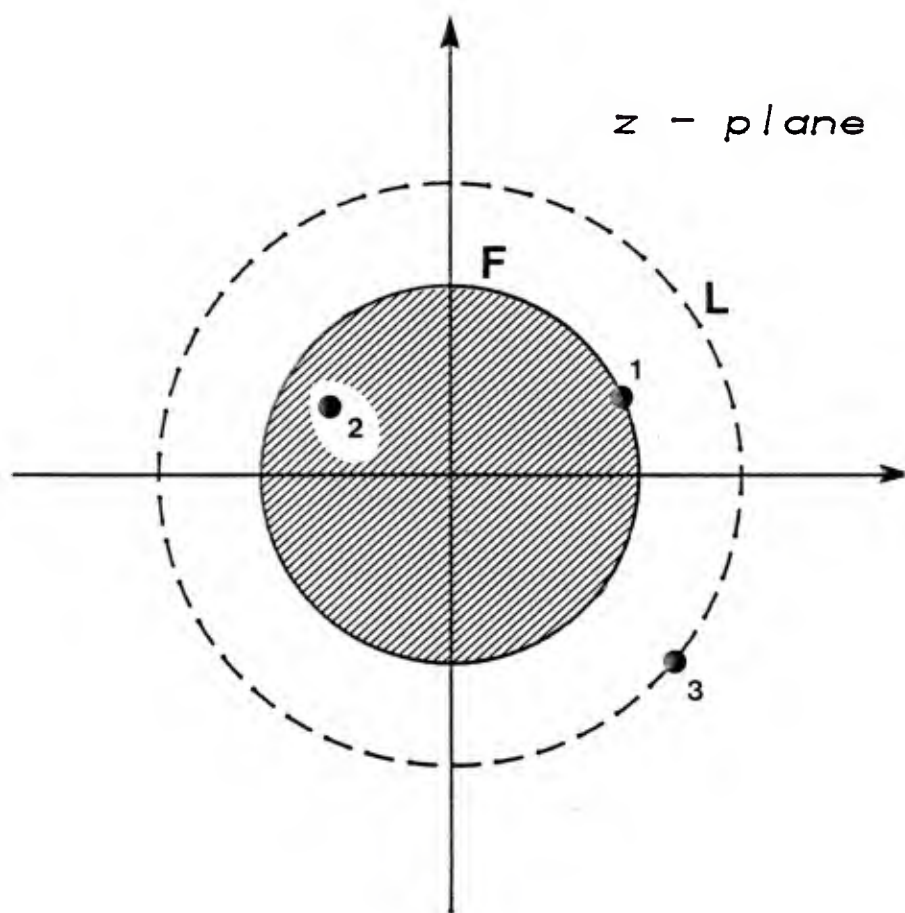


Figure A-1. Configuration of Fourier and Laplace inversion paths in complex z -plane.

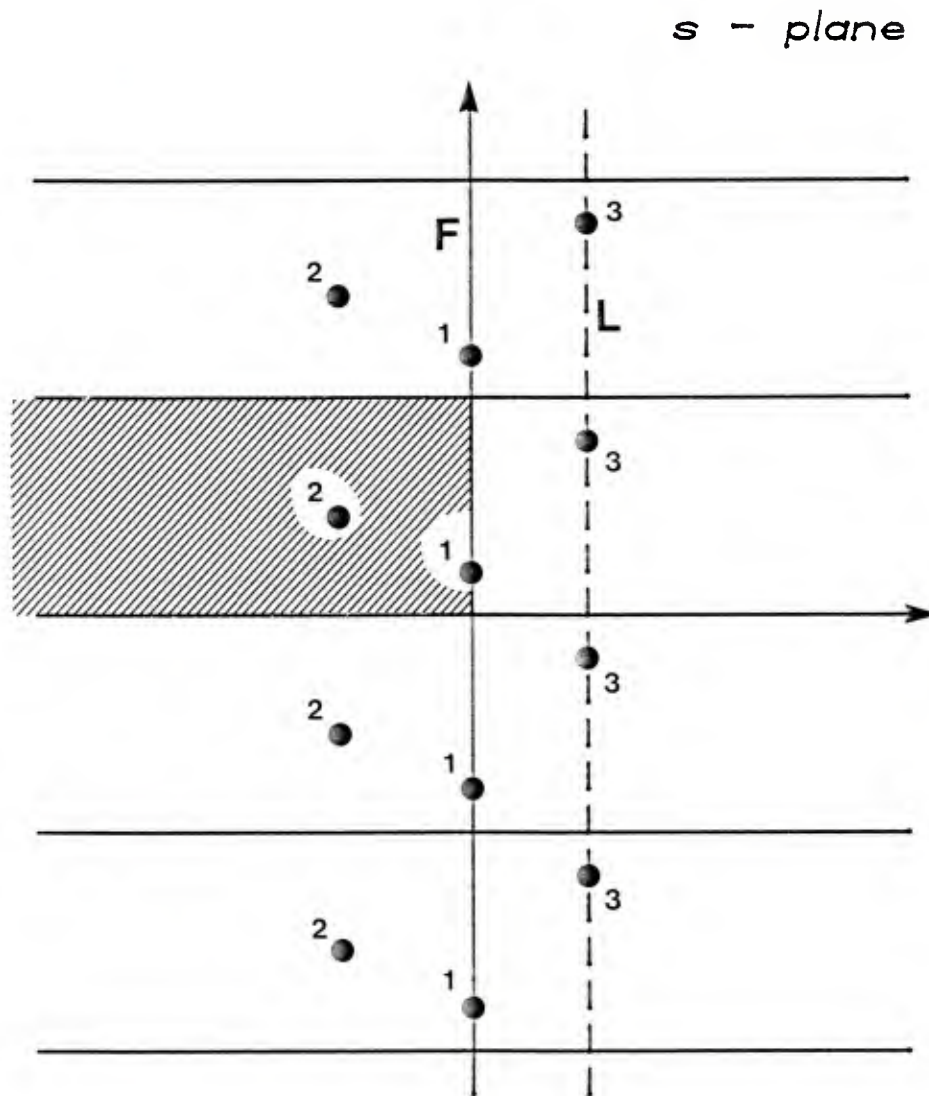


Figure A-2. Configuration of Fourier and Laplace inversion paths in complex s -plane. Shaded area and numbered points correspond to figure A-1.

REPORT NO. NADC-82253-30

APPENDIX B

COMPUTER CODE

```

1  PROGRAM TRAC5(INPUT,OUTPUT,TAPE20,TAPE40)
*****
*  TRAC5 TRACKS THE PHASE SPECTRUM OF THE INPUT
*  TIME SERIES BY FFT INTERPOLATION (1:8) AND CUBIC
*  SPLINE INTERPOLATION.
*
*  REFER QUESTIONS TO THOMAS B. GABRIELSON
*  AT THE U.S. NAVAL AIR DEVELOPMENT CENTER (CODE 3032)
*  WARMINSTER, PENNSYLVANIA 18974. (215) 441-2172
*****
COMMON PAD1(4),DATA(2050),PAD2(4),SPEC(2050),G(6,2)
COMMON /TEST/ JTAG(1025)
COMMON /CUT/ NCUT
DIMENSION DA(256), IND(150), INN(100), IREC(25)
DATA IREC/2,3,4,6,7,9,10,12,14,16,18,20,22,24,
$ 26,28,30,32,33,34,35,36,37,38,39/
CALL OPENMS(20,IND,150,0)
CALL OPENMS(40,INN,100,0)
TWOPI = 6.283185308
DO 800 IRC=1,6
  NCUT = 0 $ MA = 0
  DATA(2049) = 1.0
  IRX = IREC(IRC)
25  READ TIME SERIES
C
C
C
CALL READMS(20,DA,256,IRX)
DO 300 IJX=1,5
C
C  COMPUTE THE SIGNAL SHIFT REQUIRED TO BRING THE PHASE
C  OF THE LAST SPECTRAL POINT BACK TO ZERO. ON FIRST
C  PASS (IJX=1) NCUT=MA=0 HENCE M=0.
C
C  M = -2*NCUT + MA
C
C  NUMBER OF BRANCH CROSSINGS ESTABLISHES REQ'D SHIFT
C  TO WITHIN TWO. SIGN OF LAST POINT RESOLVES SHIFT TO
C  LAST FIGURE.
C
  IF(DATA(2049).GT.0.0) GO TO 80
  M = M - 1
80  PRINT 9000, NCUT,M,IRX,IRC
9000  FORMAT(*,NCUT,M,IRX,IRC *,4I10)
  M1 = M + 1
C
C  TRANSFER 256 TIME POINTS INTO LARGER ARRAY (FOR
C  ZERO-PADDING) SHIFTED BY M POINTS.
C
  DO 100 I=1,2050
100  DATA(I) = 0.0
  IF(IJX.EQ.1) GO TO 130
  DO 120 I=1,M
120  DATA(2048-M+I) = DA(I)
130  CONTINUE
  DO 140 I=M1,256

```

```

60      140 DATA(I-M) = DA(I)
        CALL FFT2048(DATA)
        C
        C      ADD OVERFLOW ON BOTH ENDS OF DATA (SEE STRUCTURE
        C      IN COMMON) TO ALLOW SPLINE FIT NEAR ENDS.
        C
        PAD1(1) = DATA(2047) $ PAD1(2) = DATA(2048)
        PAD1(3) = DATA(2049) $ PAD1(4) = DATA(2050)
        PAD2(1) = DATA(1) $ PAD2(2) = DATA(2)
        PAD2(3) = DATA(3) $ PAD2(4) = DATA(4)
        CALL PHASE(DA,M)
        C
        C      COMPUTE ABSOLUTE PHASE AND COMPARE WITH PREVIOUS
        C      COMPUTATION ALLOWING FOR SHIFT
        C
        ANGERR = 0.0
        SHIF = (M - MA)*TWOPI/2048.0
        C
        C      SHIF IS SHIFT PER SPECTRAL POINT.
        C
        NCA = 0 $ NCB = 0
        DO 500 I=1,1025
        ASHIF = (I-1)*SHIF + ANGERR
        X = DATA(2*I-1) $ Y = DATA(2*I)
        C
        C      COMPUTE ABSOLUTE PHASE ANGLE (SPEC(2*I) HOLDS
        C      NCUT FOR I"TH POINT.
        C
        ABSANG = ATAN2(Y,X) + SPEC(2*I)*TWOPI
        IF(IJX.EQ.1) GO TO 400
        C
        C      TAKE ABSOLUTE PHASE ANGLE VALUE FROM PREVIOUS
        C      PASS AND SHIFT ACCORDING TO TIME SERIES SHIFT
        C      BETWEEN PASSES. COMPARE THIS TO NEW ANGLE.
        C
        DIFANG = ABSANG - SPEC(2*I-1) - ASHIF.
        DDTEST = ABS(DIFANG)
        IF(DDTEST.LT.O.1) GO TO 400
        C
        C      IF THERE WAS AN ERROR BETWEEN THESE TWO COMPUTATIONS,
        C      ACCUMULATE THE ERROR.
        C
        ANGERR = ANGERR + SIGN(TWOPI,DIFANG)
        PRINT 9600,I,ABSANG,SPEC(2*I-1),DIFANG,ANGERR,JTAG(I)
        PRINT 9100,DATA(2*I-3),DATA(2*I-2),DATA(2*I-1),DATA(2*I)
        9100 FORMAT(* DATA 1. (RE IM) DATA 2 (RE IM) *4F20.4)
        C
        C      EXAMINE PROBLEM AREAS IN SAME MANNER AS PHASE
        C      SUBROUTINE.
        C
        IPRE = I - 1
        CALL CPA(P,IPRE)
        CALL DFT(P,IPRE,TR,TI,DA,M)
        NCC = 0
        CALL ACUT(DATA(2*I-3),DATA(2*I-2),TR,TI,NCC)
        CALL ACUT(TR,TI,DATA(2*I-1),DATA(2*I),NCC)
        NCX = SPEC(2*I) - SPEC(2*I-2)

```



```

115      NCA = NCA + NCC $ NCB = NCB + NCX
      C
      C NCC IS CROSSING INDEX FOR RECOMPUTATION OF PROBLEM
      C AREA. NCA ACCUMULATES THIS VALUE FOR ALL PROBLEM AREAS.
      C NCX IS CROSSING INDEX DETERMINED IN PREVIOUS PASS AND
      C NCB ACCUMULATES THIS VALUE FOR ALL PROBLEM AREAS.
      C
      PRINT 9300, NCC, NCX
      9300 FORMAT(* ACTUAL ESTIMATED *215)
      PRINT 9200
      9200 FORMAT(* *)
      400 SPEC(2*I-1) = ABSANG
      500 CONTINUE
      9600 FORMAT(* I ABSANG OLDANG (DIFANG ANGERR) *18,4F15.4,18)
      C
      C IF NCUT.EQ.0 THEN PHASE HAS BEEN PROPERLY CONSTRUCTED
      C AND THE LINEAR RAMP COMPONENT HAS BEEN REMOVED.
      C
      IF(NCUT.EQ.0) GO TO 600
      IF(IJX.EQ.1) GO TO 250
      PRINT 9400, NCUT
      9400 FORMAT(* IMPROPER PHASE RAMP COMPENSATION: NCUT =*15)
      250 MA = M
      C
      C ADJUST NCUT FOR THE SPECIAL PROBLEM AREAS DETECTED
      C IN THE "DO 500" LOOP.
      C
      NCUT = NCUT + NCA - NCB
      PRINT 9700, NCUT
      9700 FORMAT(* MODIFIED NCUT *15)
      300 CONTINUE
      600 CONTINUE
      C
      C AT THIS POINT, SPEC(EVEN INDECIES) HOLDS THE ABSOLUTE
      C PHASE ANGLE VALUES. THE MAGNITUDE VALUES CAN NOW BE
      C STORED IN SPEC(ODD INDECIES) ALTHOUGH THIS IS NOT
      C PRESENTLY DONE.
      C
      CALL WRITMS(40, SPEC, 2050, IRC)
      PRINT 9500, IRX, IRC, NCUT
      9500 FORMAT(* RECORD WRITTEN: IRX IRC NCUT *3110./)
      800 CONTINUE
      END

```

SUBROUTINE SPLINE 74/74 OPT=1 FTN 4.6+428 82/09/07. 15.51.04 PAGE 1

```

1  SUBROUTINE SPLINE(JKK)
   *****
   *
   *   SPLINE FITS SIX SPECTRAL POINTS WITH TWO CUBIC
   *   SPLINE CURVES: ONE FOR THE REAL PART AND ONE FOR
   *   THE IMAGINARY PART. THE CURVATURES ARE STORED IN
   *   THE ARRAY, G.
   *
   *****
10  COMMON PAD1(4),DATA(2050),PAD2(4),SPEC(2050),G(6,2)
   DIMENSION AS(5),FS(5),Y(6)
   I1 = 2*JKK - 8
   DO 150 IQ=1,2

   C   EXTRACT REAL (IQ=1) OR IMAGINARY (IQ=2) PART
   C
   DO 110 I=1,6
110  Y(I) = DATA(I1 + 2*I + IQ)
   J = 5 $ A = 4.0
   F = Y(6) - 2.0*Y(5) + Y(4)

   C   REDUCE EQUATIONS FROM BOTTOM UP
   C
120  AS(J) = A $ FS(J) = F $ J = J - 1
   IF(J.EQ.1) GO TO 130
   A = 4.0 - 1.0/A
   F = Y(J+1) - 2.0*Y(J) + Y(J-1) - F/A
   GO TO 120
130  G(1,IQ) = G(6,IQ) = 0.0
   GO = G(2,IQ) = FS(2)/AS(2)
   I = 3

   C   COMPUTE CURVATURES FROM TOP DOWN
   C
140  GO = G(1,IQ) = (FS(1)-GO)/AS(1)
   I = I + 1
   IF(I.LT.6) GO TO 140
150  CONTINUE
   RETURN
   END
40

```

```

1  SUBROUTINE PHASE(DA,M)
   *****
   *
   *   PHASE IS THE EXECUTIVE ROUTINE THAT TRACKS
   *   THE SPECTRAL PHASE PROGRESSION. THE BASIC CRITERION
   *   FOR TESTING ADJACENT POINTS IS A TEST FOR THE
   *   INCLUDED ANGLE. BY USING THE VECTOR DOT PRODUCT,
   *   THE COSINE OF THIS ANGLE IS FOUND AND, IF THE COSINE
   *   IS GREATER THAN ZERO (I.E., THE INCLUDED ANGLE LESS
   *   THAN 90 DEGREES), NO SPECIAL ALGORITHM IS NEEDED TO
   *   FOLLOW THE PHASE. NCUT COUNTS THE NET NUMBER OF TIMES
   *   THAT THE NEGATIVE REAL AXIS IS CROSSED IN THE POSITIVE
   *   (COUNTER-CLOCKWISE) DIRECTION.
   *****
15  *****
   COMMON /CUT/ NCUT
   COMMON /TEST/ JTAG(1025)

   C
   C   JTAG IS ONLY USED FOR TRACKING DOWN BUGS.
   C
20  COMMON /X/ X1,Y1,X2,Y2
   COMMON PAD1(4),DATA(2050),PAD2(4),SPEC(2050),G(6,2)
   DIMENSION DA(1)
   NCUT = 0
   X1 = DATA(1) $ Y1 = DATA(2)

   C
   C   TEST EACH PAIR OF SPECTRAL POINTS
   C
30  DO 600 J=1,1024
   X2 = DATA(2*J+1) $ Y2 = DATA(2*J+2)

   C
   C   CS IS DOT PRODUCT OF THE POSITION VECTORS OF POINTS
   C   X1,Y1 AND X2,Y2: A.B = /A/B/COS(PHI). IF THIS IS
   C   POSITIVE, THEN COS(PHI) MUST BE POSITIVE AND /PHI/
   C   MUST BE LESS THAN 90 DEGREES.
   C
   CS = X1*X2 + Y1*Y2
   PRINT 9100,J,X1,Y1,X2,Y2
9100  FORMAT(* J X1 Y1 X2 Y2 *I10.5X,4F10.2,F10.4)
   JTAG(J+1) = 0
   IF(CS.GT.0.0) GO TO 400

   C
   C   IF INCLUDED ANGLE (PHI).LT.90 DEGREES, CONSTRUCT SPLINE
   C   THROUGH THE SIX POINTS CENTERED ON X1,Y1 AND X2,Y2.
   C   LOCATE THE CLOSEST POINT OF APPROACH TO THE ORIGIN AND
   C   COMPUTE DFT THERE TO DETERMINE TRAJECTORY LOCATION.
   C
   CALL SPLINE(J)
   CALL CPA(P,J)
   CALL DFT(P,J,XM2,YM2,DA,M)

   C
   C   CHECK FOR CROSSING OF THE NEGATIVE REAL AXIS.
   C
300  CALL CUT(X1,Y1,XM2,YM2)
   CALL CUT(XM2,YM2,X2,Y2)
   JTAG(J+1) = 2
   GO TO 500
55  *****

```

PAGE 2

82/09/07. 15.51.04

FTN 4.6+428

74/74 OPT=1

SUBROUTINE PHASE

```

C
C      CHECK FOR CROSSING OF THE NEGATIVE REAL AXIS.
C
60    400 CALL CUT(X1,Y1,X2,Y2)
      500 CONTINUE
C
C      STORE NUMBER OF CROSSINGS UP TO J+1"TH POINT.
C
65    SPEC(2*J+2) = NCUT
      X1 = X2 $ Y1 = Y2
      600 CONTINUE
      RETURN
      END
70

```

```

1  SUBROUTINE CUT(X1,Y1,X2,Y2)
   *****
   * CUT TESTS A PAIR OF SPECTRAL POINTS TO DETERMINE
   * IF THE NEGATIVE REAL AXIS HAS BEEN CROSSED AND, IF SO,
   * WHAT THE DIRECTION OF CROSSING IS. THE CASE OF
   * Y1 = Y2 = 0 HAS BEEN IGNORED.
   * *****
   * *****
10  COMMON /CUT/ NCUT
   C
   C SINCE INCLUDED ANGLE MUST BE .LT.90 DEGREES, NO
   C CROSSING IS POSSIBLE IF EITHER POINT IS IN RIGHT
   C HALF PLANE.
15  C
   IF (X1.GT.O.O.OR.X2.GT.O.O) RETURN
   P = Y1*Y2
   IF (P.GT.O.O) RETURN
   IF (P.LT.O.O) GO TO 100
   IF (Y1.GT.O.O.OR.Y2.GT.O.O) RETURN
   100 NCUT = NCUT + 1
   IF (Y1.LT.Y2) NCUT = NCUT - 2
   C PRINT 9000,NCUT
   9000 FORMAT(* BRANCH CROSSING DETECTED: NCUT +I10)
   C RETURN
   END
25

```

SUBROUTINE CPA 74/74 OPT=1 FTN 4.6+428 82/09/07. 15.51.04 PAGE 1

```

1      SUBROUTINE CPA(P,J)
      *****
      *
      *      CPA LOCATES THE PARAMETER VALUE OF THE APPROXIMATE
      *      CLOSEST POINT OF APPROACH OF THE SPLINE SEGMENT.
      *
      *****
      D1 = DIST(O.O,J) $ D2 = DIST(1.O,J)
      C
      C      P (AND FIRST ARGUMENT OF DIST) IS LOCATION PARAMETER
      C      ALONG CURVE BETWEEN POINTS J AND J+1.
      C
      DELP = 0.25 $ P = 0.5
      DO 200 IQ=1,10
      C
      C      LOCATE SMALLEST DISTANCE TO ORIGIN BY BISECTION.
      C
      C
      C      PRINT 9000,D1,D2,P
      IF(D1.LT.D2) GO TO 100
      D1 = DIST(P,J) $ P = P + DELP
      GO TO 150
      100 D2 = DIST(P,J)
      P = P - DELP
      150 DELP = DELP/2.0
      200 CONTINUE
      9000 FORMAT(* D1 D2 P *3F20.4)
      RETURN
      END

```



```

1      FUNCTION DIST(P,J)
      *****
      *
      *      DIST FINDS THE (DISTANCE)**2 TO THE ORIGIN OF
      *      A POINT ON A SINGLE SPLINE SEGMENT.
      *
      *****
      COMMON PAD1(4),DATA(2050),PAD2(4),SPEC(2050),G(6,2)
      TB = P $ TA = 1.0 - TB
      X = TA*G(3,1)*(TA*TA-1.0) + TB*G(4,1)*(TB*TB-1.0)
      $      + TA*DATA(2*J-1) + TB*DATA(2*J+1)
      Y = TA*G(3,2)*(TA*TA-1.0) + TB*G(4,2)*(TB*TB-1.0)
      $      + TA*DATA(2*J) + TB*DATA(2*J+2)
      DIST = X*X + Y*Y
      RETURN
      END
15

```

PAGE 1

82/09/07. 15.51.04

FTN 4.6+428

SUBROUTINE DFT 74/74 OPT=1

```

1  SUBROUTINE DFT(P,J,TR,PI,DA,M)
   *****
   *
   *      DFT COMPUTES THE DISCRETE FOURIER TRANSFORM
   *      AT THE LOCATION SPECIFIED BY J AND P.
   *
   *****
   DIMENSION DA(4)
   TWOPI = 6.283185308
   PRINT 9100,P,J
   9100 FORMAT(* P J (DFT) *F20.4,I10)
   A = (J-1) + P
   TANG = TWOPI*A/2048.0
   CSN = 1.0 $ SNE = 0.0
   DC = COS(TANG) $ DS = SIN(TANG)
   DRE = 0.0 $ DIM = 0.0

15  C      PERFORM DFT ON UNSHIFTED TIME SERIES
   C
   C      DO 500 N=1,256
   C
   C      ADD NEXT TERM IN DFT SERIES
   C
   DRE = DRE + DA(N)*CSN
   DIM = DIM - DA(N)*SNE
   C
   C      UPDATE SIN AND COS OF ANGLE ROTATED BY TANG.
   C
   CXE = CSN*DC - SNE*DS
   SNE = SNE*DC + CSN*DS
   CSN = CXE
   500 CONTINUE
   C
   C      COMPENSATE FOR SHIFT IN TIME SERIES
   C
   PHI = M*TANG
   PR = COS(PHI) $ PI = SIN(PHI)
   TR = DRE*PR - DIM*PI
   TI = DRE*PI + DIM*PR
   PRINT 9000,DRE,DIM,PR,PI,TR,PI
   9000 FORMAT(* DRE DIM PR PI TR TI *6F15.4)
   RETURN
   END

```

```

1  SUBROUTINE ACUT(X1,Y1,X2,Y2,NCC)
   *****
   *
   *      ACUT TESTS A PAIR OF SPECTRAL POINTS TO DETERMINE
   *      IF THE NEGATIVE REAL AXIS HAS BEEN CROSSED AND, IF SO,
   *      WHAT THE DIRECTION OF CROSSING IS.  THE CASE OF
   *      Y1 = Y2 = 0 HAS BEEN IGNORED.  THIS ROUTINE DIFFERS FROM
   *      CUT ONLY IN THAT THE GLOBAL COUNTER NCUT IS NOT
   *      MODIFIED.
   *
10  *****
   *****
   IF(X1.GT.O.O.OR.X2.GT.O.O) RETURN
   P = Y1*Y2
   IF(P.GT.O.O) RETURN
   IF(P.LT.O.O) GO TO 100
   IF(Y1.GT.O.O.OR.Y2.GT.O.O) RETURN
   100 NCC = NCC + 1
   IF(Y1.LT.Y2) NCC = NCC - 2
   PRINT 9000,NCC
   C 9000 FORMAT(* BRANCH CROSSING DETECTED: NCC *I10)
   RETURN
   .END

```

REPORT NO. NADC-82253-30

	No. of Copies
Defence Research Centre Salisbury, Adelaide, SA, Australia	1
Defence Scientific Establishment HMNZ Dockyard Auckland 9, New Zealand (Dr. K.M. Guthrie)	1
DTIC	12

REPORT NO. NADC-82253-30

	No. of Copies
Applied Physics Laboratory The John Hopkins University John Hopkins Road Laurel, MD 20707	1
Lamont-Doherty Geological Observatory Palisades, NY 10964	1
Woods Hole Oceanographic Institution Woods Hole, MA 02543	1
Scripps Institute of Oceanography Marine Physics Laboratory San Diego, CA 92152	1
Auditory Research Laboratory Northwestern University 2299 Sheridan Road Evanston, IL 60201 (Dr. Frederic Wightman)	1
Mayo Medical School Rochester, MN 55901 (Dr. James Greenleaf)	1
Canadian Superior Oil Ltd. Three Calgary Place 355-4th Avenue SW Calgary, Alberta T2P 0J1 (Dr. R. Hinds)	1
Defence Research Establishment, Pacific Forces Mail Office Victoria, BC Canada VOS 1B0	1
Defence Research Establishment, Atlantic Forces Mail Office Halifax, NS Canada	1
Admiralty Underwater Weapons Establishment Portland, Dorset, England, UK	1
Admiralty Research Laboratory Teddington, England, UK	1
Royal Aircraft Establishment Farnborough, Hants, England, UK	1
Royal Australian Naval Research Laboratory Edgehill Road Sydney, NSW, Australia	1

DISTRIBUTION LIST
TASK AREA NO. ZR 01108

	No. of Copies
CNM	
(1 for-ASW-01)	9
(1 for-ASW-10)	
(1 for-ASW-13)	
(3 for-MAT-0721)	
(3 for-MAT-0812)	
NAVAIRSYSCOM (OOD4)	6
(2 for retention)	
(1 for-AIR-340)	
(1 for-AIR-950D)	
(1 for-AIR-54902B)	
(1 for=PMA-264)	
ONR-102-OS	1
NAVELEXSYSCOM-PME-124	1
Naval Postgraduate School (Prof. O. Heinz)	1
NOSC-714	1
NORDA-320	1
NRL-8100	1
NUSC, New London	1
SACLANT ASW Research Centre Viale San Bartolomeo 400, I-19026 La Spezia, Italy	1
Applied Research Laboratory The Pennsylvania State University P.O. Box 30 State College, PA 16801 (Dr. S.T. McDaniel; Dr. L. Sibul; library)	3
Applied Research Laboratory The University of Texas P.O. Box 8019 Austin, TX 78712	1
Applied Physics Laboratory University of Washington 1013 NE 40th Street Seattle, WA 98195	